A computational study of density-dependent individual movement and the formation of population clusters in two-dimensional spatial domains

Ellis, John; Petrovskaya, Natalia

DOI:
10.1016/j.jtbi.2020.110421

Document Version
Peer reviewed version

Citation for published version (Harvard):
Ellis, J & Petrovskaya, N 2020, 'A computational study of density-dependent individual movement and the formation of population clusters in two-dimensional spatial domains', *Journal of Theoretical Biology*, vol. 505, 110421. https://doi.org/10.1016/j.jtbi.2020.110421

A computational study of density-dependent individual movement and the formation of population clusters in two-dimensional spatial domains

John R. Ellis[a*], Natalia B. Petrovskaya[a]

[a] *School of Mathematics, University of Birmingham, Birmingham, UK*

Abstract

The patterns of collective behaviour in a population emerging from individual animal movement has long been of interest to ecologists, as has the emergence of heterogeneous patterns among a population. In this paper we will consider these phenomena by using an individual based modelling approach to simulate a population whose individuals undergo density-dependent movement in 2D spatial domains. We first show that the introduction of density-dependent movement in the form of two parameters, a perception radius and a probability of directed movement, leads to the formation of clusters. We then show that the properties of the clusters and their stability over time are different between populations of Brownian and non-Brownian walkers and are also dependent on the choice of parameters. Finally, we consider the effect of the probability of directed movement on the temporal stability of clusters and show that while clusters formed by Brownian and non-Brownian walkers may have similar properties with certain parameter sets, the spatio-temporal dynamics remain different.

Keywords: animal movement, individual-based modelling, Brownian motion, density-dependence, pattern formation

1. Introduction

Spatial distributions of animal and plant taxa are often distinctly heterogeneous [30, 45]. The phenomenon of spatial aggregation also known as patchiness [30, 46], clustering [20, 35, 89] or, more generally, ecological pattern formation [65], is important in many areas of ecological research. There are many drivers behind formation of spatially aggregated structures in the population. Spatial aggregation is important for reproduction [16, 17, 87, 98], in prey-predator interactions [34, 26, 60, 74, 82, 94], and competition [10, 33, 63, 91]. There have also been numerous studies that have found populations congregating for foraging and hunting [13, 23, 78, 86], thermo-regulation [7, 27], or for purely social reasons [8, 22].

Among all varieties of factors responsible for spatial aggregation, interorganismal interactions can play a dominant role when spatial clusters of animal species are formed at small

*Corresponding author

Email address: jxe348@student.bham.ac.uk (John R. Ellis[a])

spatial scales, e.g. within a particular forest, lake, meadow or agricultural field [1, 36, 43, 59, 64, 68]. Such heterogeneous spatial distributions are related to smaller time scales where reproduction and other interactions are not involved. There are different mechanisms that have been identified to cause small time scale pattern formation in populations, one of them being the response of individual animals to the presence of their conspecifics [98]. Some populations aggregate as a consequence of animal 'sociality' [31, 32] and modify their movement based on movement characteristics of their close neighbours as seen in flocks, herds or swarms [32, 43, 77]. Patterns of high population density have also shown to be formed by a change in the speed of movement with density whereby an animal moving into a higher density area will slow down causing clusters [48, 49]. Other animals will simply be more inclined to move towards their conspecifics and aggregate as a consequence of this density-dependent movement [41, 49, 56, 89, 90].

While the density-dependent movement of individual animals is known to influence the spatial distribution of populations of some species with the mechanisms mentioned above, it is still unclear how local biotic interactions in certain species lead to spatial aggregation of the population. One example that has partially motivated our work is spatial distribution of grey field slug *Deroceras reticulatum* in agricultural fields. Slug patches (i.e. spatial sub-domains with high slug density) have been shown to have a sufficiently stable spatio-temporal distribution [2, 6, 24], yet the relative importance of biotic factors in determining the spatial distribution of slugs within one generation on a spatial scale of arable field remains an open question. There is some empirical evidence that movement of slugs exhibits density-dependence as individual slugs respond to the presence of their conspecifics by following their trails [97] and further experimental and theoretical study is required to investigate the hypothesis of density-dependent movement in slug populations. As slugs are among the most dangerous pests in agriculture, development of a comprehensive modelling framework with strong predictive capacity and flexible enough to incorporate various types of density-dependent movement should help with better understanding of mechanisms of spatial heterogeneity which, in turn, will lead to more informed monitoring and control decisions.

For small-scale, within-generation spatial patterns formed as a result density-dependent movement, the process of pattern formation in a population can be modelled by simple interactions between individuals resulting in the emergence of collective behaviour [88]. In this paper we consider a stochastic model for two-dimensional (2D) individual-based movement which includes a density-dependent directional bias. Our aim is to then analyse the spatio-temporal population dynamics and understand how the degree of spatial aggregation in the population is determined by the type of individual movement. Our approach to modelling 2D density-dependent movement is partly based on our previous work [20] where formation of spatial clusters has been confirmed for 1D density-dependent movement. Meanwhile, the results obtained in the 1D model cannot be directly extended to a more realistic 2D case with more sophisticated rules of individual movement. Several new important questions arise, the definition of a 2D spatial cluster being one of them. The importance of accurate quantification of ecological spatial patterns has been acknowledged by scientists since long ago [28, 45, 37] and it is clear that an irrelevant definition of a spatial cluster may result in irrelevant conclusions

about the spatio-temporal population dynamics. Hence we design carefully the concept of a spatial cluster when our model is developed. Our definition incorporates two basic principles of cluster identification - measuring the distance to the nearest neighbour [14] and measuring the number of neighbours within a spatial unit [50] - to help us to analyse quantitative properties of the spatio-temporal dynamics such as number of clusters, the mean cluster area, and the mean population within the cluster. Based on our definition of a spatial cluster we compare the results of the 2D model with the previous 1D model [20] to demonstrate that, while density-dependent movement in 2D domains is responsible for cluster formation, it results in much more complex spatio-temporal dynamics.

Another question we are concerned with is how the quantitative properties of spatial distribution respond to a change in the parameters of directed movement. The investigation of this question is important as it allows one to conclude on whether the process responsible for spatial pattern formation can be at least to some degree identified and understood by pattern analysis on its own [38, 54, 69]. The two cases we study in the paper are where animals perform Brownian motion (i.e. described by a Gaussian dispersal kernel) [40, 83] and non-Brownian motion (described by a power law dispersal kernel) [93]. We therefore analyse how the spatio-temporal dynamics of the population distribution depend on key parameters in our model, i.e. the probability of directed movement and the perception radius, for both Brownian and non-Brownian walkers. The concept of the temporal stability of population clusters is introduced and we argue that the analysis of spatial distributions alone may not be sufficient to conclude about the movement type. It will be shown in the paper that, while the spatial distributions of Brownian walkers and non-Brownian walkers can be indistinguishable when considering quantification of spatial clusters, their spatio-temporal dynamics are still different.

The paper is organised as follows. In Section 2, we outline the rules of the model and introduce density-dependent movement. The definition of a cluster will be explained and validated to provide a reliable framework for further analysis. We justify our choice of parameters of directed movement in Section 3 and present the results of simulations of Brownian walkers with that parameter set. We then proceed to discuss the results of simulations of non-Brownian walkers with an 'equivalent' parameter set to allow for further comparison between Brownian and non-Brownian movement. Proceeding from this we directly compare results from simulations of Brownian walkers and non-Brownian walkers in Section 4. Finally, we offer discussion of the results and our conclusions in Section 5.

2. Model of density-dependent movement

To simulate density-dependent animal movement in a 2D domain we use the individual-based modelling approach[1] [11, 29, 39, 88]. We closely follow the methods developed previously in our 1D model [20]. For simulation of density-dependent random movement the position of

[1]To facilitate reproducibility and date re-use, we have made the computer code used to generate our results available in a repository [21].

each individual is given at a discrete moment in time t_k, $k = 0, 1, ..., t_{k+1} = t_k + \Delta t$ where Δt is the time increment. In this paper we consider $\Delta t = 1$ for all time steps; for simplicity we drop the k and refer to t as the series of integers that are discrete time steps.

For a population of N animals, the location of the n_{th} animal at time t is given by $(x_n(t), y_n(t))$. If this is known, the position at time $(t + 1)$ is simulated as

$$(x_n(t+1), y_n(t+1)) = (x_n(t) + \Delta x, y_n(t) + \Delta y), \tag{1}$$

where $\Delta x,\ \Delta y$ are the spatial increments that the animal moves in the x and y direction respectively during the time increment $\Delta t = 1$. The movement of animal n starts from an initial position $(x_n(0), y_n(0)) = (x_{n,0}, y_{n,0})$.

As the step size will be the radial distance an animal moves to from its previous position, it is convenient consider the movement in terms of polar coordinates, (r, θ) with the centre at $(x_n(t), y_n(t))$. To define the increments $\Delta x,\ \Delta y$, we consider the radial distance $\Delta r = \sqrt{(\Delta x)^2 + (\Delta y)^2}$ that an animal will move during one time step and the direction θ in which the step is made. Therefore the change in x and y of the position of an individual at any given time step is given by

$$\Delta x = (\Delta r)cos(\theta), \quad \Delta y = (\Delta r)sin(\theta). \tag{2}$$

Following [15, 39, 88], we consider Δr to be a random variable distributed according to a certain probability density function $\rho(\Delta r)$ which we refer to as the dispersal kernel. For simplicity, we assume all animals in a population have identical movement behaviour so ρ is the same for all animals.

Since we are studying the spatial patterns of the population arising from different rules of individual movement, in particular Brownian and non-Brownian motion, we consider two cases. In the first case, the dispersal kernel is a normal distribution with a mean of 0 and a variance σ^2:

$$\rho(\Delta r) = \rho_G(\Delta r|0, \sigma^2) = \frac{1}{\sqrt{2\pi\sigma^2}} \exp\left(-\frac{(\Delta r)^2}{2\sigma^2}\right). \tag{3}$$

We note here that, as the radial distance an animal moves must be non-negative, we use a half-normal distribution in our computer simulations:

$$\rho(\Delta r) = \rho_G(\Delta r|0, \sigma^2) = \begin{cases} \frac{2}{\sqrt{2\pi\sigma^2}} \exp\left(-\frac{(\Delta r)^2}{2\sigma^2}\right) & \text{if } \Delta r \geq 0, \\ 0 & \text{if } \Delta r < 0. \end{cases} \tag{4}$$

Where σ is the standard deviation of the original normal distribution. The distribution (4) is a special case of the folded normal distribution and has a mean μ_f and standard deviation σ_f given by

$$\mu_f = \sigma\sqrt{\frac{2}{\pi}}, \quad \sigma_f = \sigma\sqrt{1 - \frac{2}{\pi}}. \tag{5}$$

However, we also need the baseline definition (3) when a comparison with the results of our 1D study is made further in the paper. We will refer to animals performing movement described by Eqn. (3) as Brownian walkers.

In the second case, the dispersal kernel is given by the power law:

$$\rho(\Delta r) = \rho_P(\Delta r|k,\gamma) = \frac{C}{(k+\Delta r)^{\gamma}}, \tag{6}$$

where $k > 0$ and $\gamma > 0$ are parameters of the distribution and $C = 0.5(\gamma-1)k^{\gamma-1}$ is the normalising coefficient, i.e. $\int_{-\infty}^{\infty}\rho(\xi)d\xi = 1$. Animals performing movement described by Eqn. (6) will be referred to as non-Brownian walkers further in the text.

The formulation of Δr follows the same framework as the calculation of the step size Δx in our 1D model [20], however the direction of movement given by the variable θ in a 2D domain will be different. For a non-density-dependent random walk, θ would be considered to be a random variable distributed according to a uniform distribution in the region $[0, 2\pi]$. In our model, the definition of θ will have to be adjusted to include density-dependent movement, the mechanism for which is introduced in the next section.

We consider movement in a closed domain of size $L_x \times L_y$ so that, for any n, $0 < x_n(t) < L_x,\ 0 < y_n(t) < L_y$ for all t. In this paper we consider a square domain so that $L_x = L_y = L$ The closed boundaries are modelled by introducing an additional rule. Let the value of Δx or Δy generated for the $(n+1)$th step be such that either $x_n(t+1) < 0$, $x_n(t+1) > L$, $y_n(t+1) < 0$ or $y_n(t+1) > L$. Then this step is aborted, hence effectively changing the animal's decision to leave, and a new Δr and θ are generated to make sure that the animal remains inside the domain, i.e. $0 < x_n(t+1),\ y_n(t+1) < L$.

For the initial condition, we consider a population distribution that is uniform over the 2D domain. This involves generating the initial coordinates of each individual in the x and y direction using the probability density functions $\rho_{x0}(x)$ and $\rho_{y0}(y)$ which are both independent on space; $\rho_{x0} = \rho_{y0} = 1/L = const.$

2.1. Density-dependent movement

So far we have described a simulation procedure of independent animal movement where the movement of an individual is not dependent on the location of their conspecifics. This procedure is similar to those used in many other studies of spatio-temporal population dynamics [71, 83, 88]. Having constructed this model, we can now make adjustments so that the direction of movement θ of an individual is dependent on the position of other animals in their vicinity, thereby introducing density-dependence.

To account for this, we introduce a 'perception radius' $R \geq 0$ [75, 81]. This is the distance in any direction that an individual can detect the presence of other animals. Only those animals within the perception radius at time t can affect the movement of the individual. This is illustrated in Fig. 1(a), where the perception radius is shown as the dotted circle around the individual in red.

Once the perception radius R has been introduced, the next step is to identify regions with high population density within a circular domain defined by R. In our model, this is achieved by splitting a circle of radius R around an individual into S segments of equal size. The number of neighbouring individuals in each segment is then counted to give the population

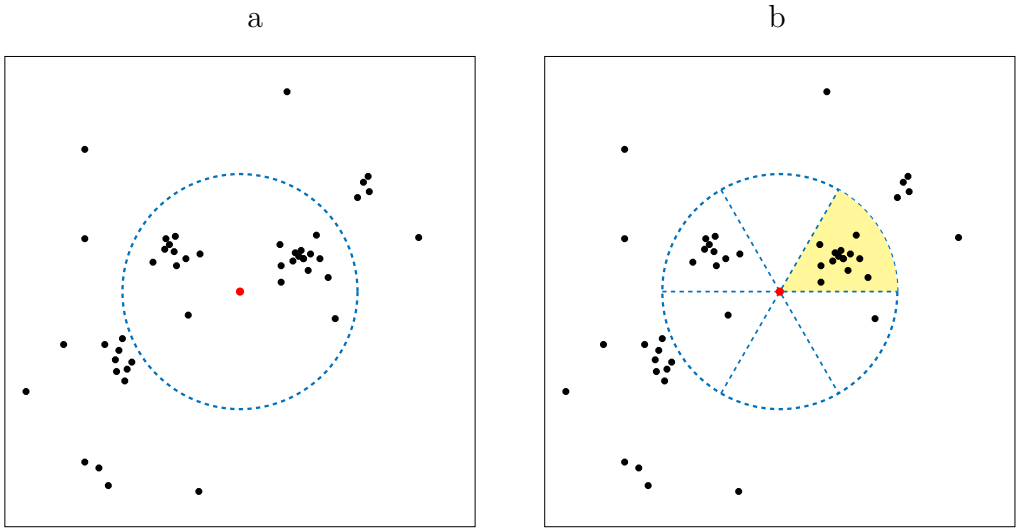

Figure 1: *(a) An individual (shown in red) can detect the presence of other individuals within a circular domain defined by the perception radius, (b) the area within the perception radius split into segments with the most populated segment highlighted.*

within the segment and therefore to find the segment s^* with the largest population m_s. The mean angle θ_d of neighbours within only the segment s^* is then calculated as

$$\theta_d = \frac{\sum_{i=1}^{m_s} \theta_{n,i}}{m_s}, \tag{7}$$

where $\theta_{n,i}$ is the angle between animal n and animal i, (x_n, y_n) are the coordinates of the animal whose direction of movement we are calculating, and $(x_i, y_i),\ i = 1, ..., m_s$ are the coordinates of all neighbours within the segment s^*. Hence, θ_d is the angle of directed movement - the direction an animal will move if it 'decides' to move towards its conspecifics. An example is shown in Fig. 1(b) where the highlighted section is the one with the largest number of neighbours. The animal will move towards the centre of the neighbours in the highlighted segment. If more than one segment has the joint largest population then one of those segments is chosen with equal probability between them.

The number of segments S is a convenient parameter in our model as it allows us to avoid ambiguous cases when the direction of individual movement has to be determined. A detailed discussion of the number of segments is provided in appendix Appendix A.1 where our choice of the value of S is explained.

We now introduce a second parameter $P \in [0, 1]$ to quantify the strength of the directional bias. Let u be an auxiliary random variable which is uniformly distributed over the interval Ω,

$$\Omega = [P - 1, P]. \tag{8}$$

For undirected movement of a given individual, we introduce a variable θ_r, which has a uniform distribution over the region $[0, 2\pi]$. If the individual animal performs directed movement, we

use the angle θ_d in (7). The direction of movement is then defined as follows:

$$\theta = \begin{cases} \theta_d, & \text{if } u \geq 0. \\ \theta_r, & \text{if } u < 0. \end{cases} \tag{9}$$

If $P = 1$ then the probability density function of u will be uniform in the region $[0, 1]$ and therefore $\theta = \theta_d$, meaning an animal will always move towards an area of high density. Conversely, if $P = 0$ then the probability density function of u will be uniform in the region $[-1, 0]$ and therefore $\theta = \theta_r$, meaning an animal will move with a random walk independent of its conspecifics. In our study we consider $0 < P < 1$ so that there is always a degree of randomness in the direction of movement, i.e. an animal will sometimes 'ignore' its conspecifics and move in a completely random direction. Thus we refer to the parameter P as the probability of directed movement.

2.2. Cluster definition

The overall aim of our study is to analyse the dynamics of population clusters as a function of the movement parameters. Clusters can be loosely thought of as spatial sub-domains with higher population density than in surrounding sub-domains. Hence we have to approximate the population density from information we have about each individual in the domain before we develop a more formal definition of a cluster. Possible methods for extracting information about the population densities from individual coordinates include the use of a Voronoi diagram [3, 85] or kernel density estimation [12, 66, 79, 96]. However these methods may not provide any extra insight into the cluster properties (e.g. average cluster area, average cluster population, etc.) as required for our study of spatio-temporal dynamics. We therefore employ the method of 'bins' previously used in our 1D model [20]. We partition the domain into a uniform square grid of BxB spatial sub-domains (bins) so that the length of a bin is L/B where L is the length of the domain. The number of animals inside a given bin divided by the area of the bin will then approximate the population density within the bin.

We then say that a group of bins form a cluster if the following conditions hold:

- For a given parameter b_u, where $0 < b_u < 1$, there is a bin that contains a proportion of the total population that is larger than b_u.
- Any bin adjacent to a bin that forms part of a cluster also belongs to the cluster if it is greater than or equal to a second parameter b_l, where $0 < b_l < b_u$.

One example of cluster identification above is shown in Fig. 2(a) where bins that form a cluster are shown as shaded areas in the domain. The number of clusters in the domain along with the cluster area (size) and population size within the cluster are useful properties for comparing cluster formation with different parameter sets in the model. These properties were calculated in the 1D model [20] so comparison between the two models can also be made. We use the MATLAB software [19, 53] to analyse cluster properties. One example is given in Fig. 2(b) where the 'boundary' function in MATLAB is employed to ascertain the size of 2D

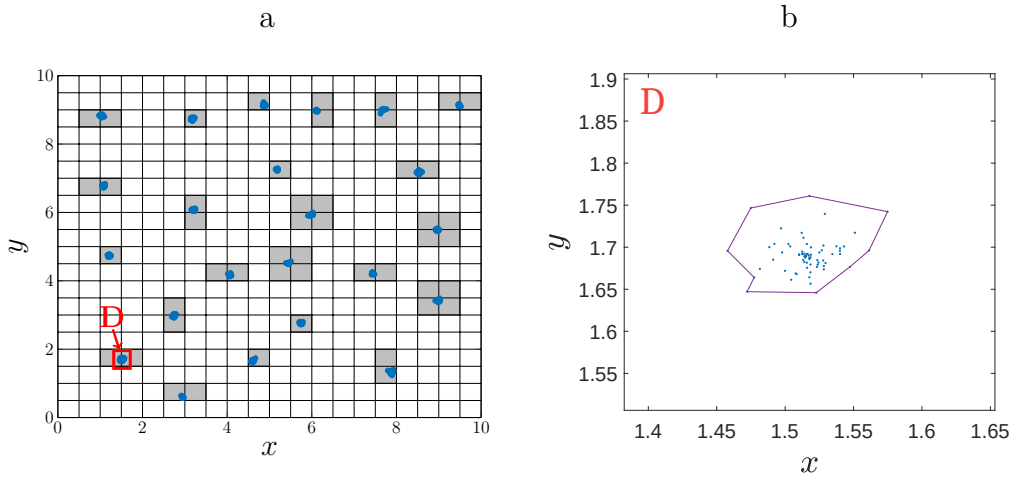

Figure 2: *(a) The domain split into* 20×20 *bins with cluster-forming bins shaded and (b) An example of the boundary of a single cluster in region D.*

cluster. The population of each cluster is calculated based on the sum of bin populations for bins that contain a cluster.

We note that the number of bins B is an arbitrary parameter in our definition of cluster. The bin size has to be chosen as it is sufficiently small so to allow for low density bins to be found between clusters, i.e. clusters do not 'merge' together. It has also to be sufficiently large so that individuals that fluctuate to small distances away are still included as part of the clusters. We therefore study how the number of clusters in the domain is effected by our choice of the number of bins. Namely, we consider how the number of clusters will change if we use a different number of bins to identify clusters in the same spatial distribution. One example of the number of clusters along with the mean cluster population when changing the number of bins is shown in Fig. 3. It can be seen from the figure that the number of clusters and the cluster population become insensitive to the choice of the number of bins B when $B \geq B^*$, where $B^* = 20$ in this example. Furthermore, the results of our computational study (see appendix Appendix A.2) reveal that, although a different choice of parameters in the problem will result in slightly different properties of the cluster, the threshold number of bins B^* remains the same and the number of clusters does not change if a $B^* \times B^*$ grid of bins is further refined.

Once the number of bins B has been defined, we choose the cluster thresholds based on the requirement that, for a cluster to be counted, there must be a bin with at least double the average bin population density and the cluster ends when a bin is reached which is below the average density. This allows most areas of high population density to be identified without noise significantly affecting the results. Since the average bin population density can be estimated as N/B^2 on a grid of $B \times B$ bins, we define $b_u = 2N/B^2$ and $b_l = N/B^2$.

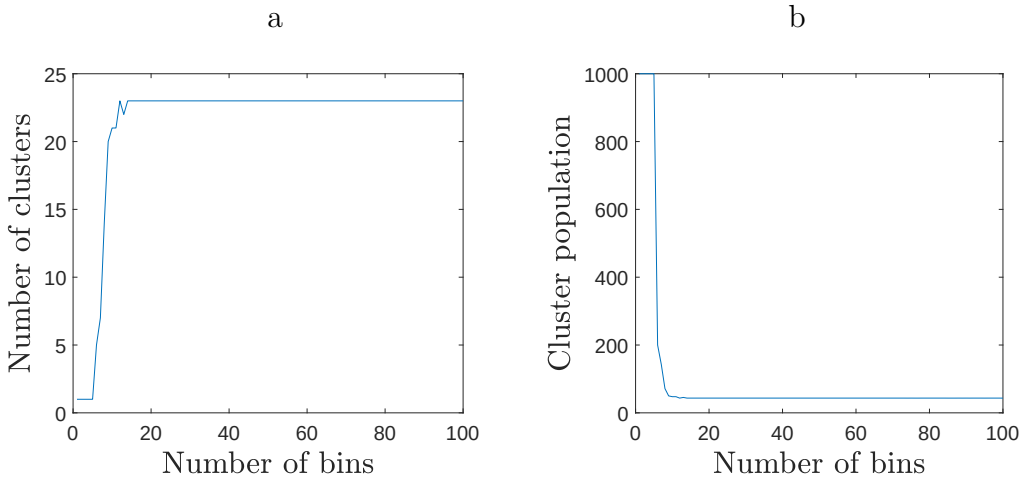

Figure 3: *Sensitivity of the definition of cluster to the choice of the number of bins. The spatial distribution of the population of of Brownian walkers (3) is analysed at time* $t = 1000$*. The simulation parameters are* $L = 10$*,* $N = 1000$*,* $P = 0.6$*,* $\sigma = 0.02$*, and* $R = 1$*. The threshold number of bins is* $B^* = 20$*: the number of clusters and the mean cluster population do not change when a grid of* $B^* \times B^*$ *bins is further refined. (a) The number of clusters and (b) the mean cluster population when changing the number of bins (squared) when identifying clusters.*

3. Simulation results

In this section we study the properties of the spatial distribution of a population where the individuals perform density-dependent random movement. We particularly want to examine how the properties of the spatial distribution change subject to the type of random movement as defined by the dispersal kernel (3) or (6), and the choice of the controlling parameters for density-dependent movement, i.e. the perception radius R, and the probability of directed movement P.

For the rest of this paper, in our simulations we consider a square domain with length $L = 10$ and the total population size $N = 10000$. We use a 20×20 grid of bins in all simulations discussed in this paper (see Section 2.2). Our choice of $B = 20$ results in cluster thresholds $b_u = 50$ (i.e 0.5% of the total population N) and $b_l = 25$ (i.e 0.25% of N). We also note that the variance σ^2 in the dispersal kernel (3) we use in our simulations has to be small compared to L so that the boundary conditions do not dominate the dynamics. Similarly the perception radius R must be smaller than L but bigger than the typical step size to allow for several clusters to form. If R is too large in comparison to L then each animal will be influenced by the majority of the rest of the population and all animals will congregate in a single cluster in the centre of the domain. Alternatively, if R is too small in comparison to the typical step size, each animal will only be influenced by few others and in the subsequent time step is likely to have moved to an area where entirely different con-specifics are now influencing their movement, never allowing clusters to form. This is discussed in more detail with specific examples further below.

Typical simulation results are shown in Fig. 4 for Brownian walkers and Fig. 5 for non-Brownian walkers. The density-dependent movement parameters used are $P = 0.6$, $R = 1$.

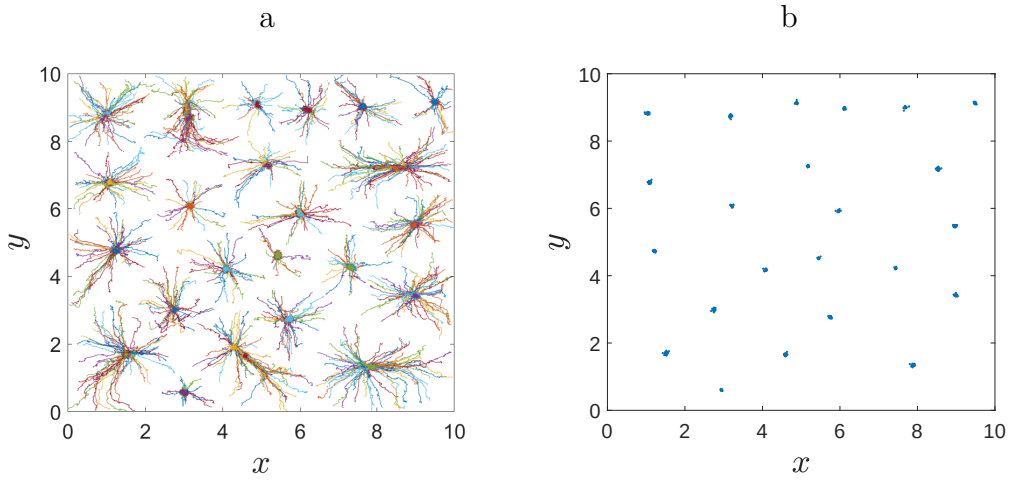

Figure 4: *Examples of the (a) individual animal paths over 1000 time steps and (b) final distribution of animals after 1000 time steps of a simulation of a population of Brownian walkers.*

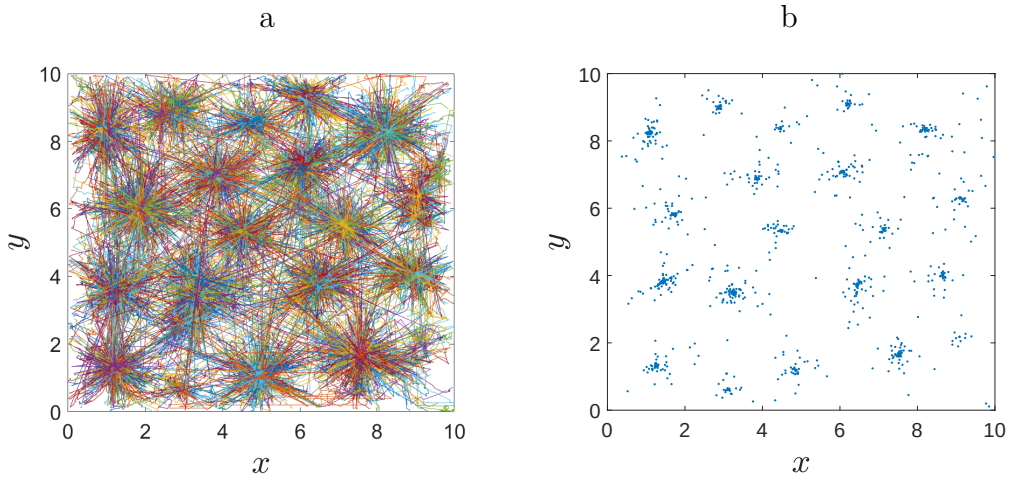

Figure 5: *Examples of the (a) individual animal paths over 1000 time steps and (b) final distribution of animals after 1000 time steps in a simulation of a population of non-Brownian walkers.*

For Brownian walkers we use the normal distribution kernel (3) with $\sigma = 0.02$, and for the non-Brownian walkers we use the power law distribution kernel (6) with $\gamma = 2,\ k = 0.0036$. In both cases the density-dependent individual movement has resulted in the formation of a number of clusters. In the case of Brownian walkers, all individuals converge to points in the domain as can be seen in Fig. 4(a) where individual animal paths are shown. The formation of distinct clusters as time progresses is shown in Fig. 4(b). In the case of non-Brownian walkers, it is possible to see some of the large step sizes in Fig. 5(a) which are characteristic of the power law dispersal kernel. Therefore clusters are not so visually distinct as in the Brownian walkers case but there are still several clusters that emerge as shown in Fig. 5(b). Hence we further examine how the type of motion and the parameter values change the number of clusters formed in the domain and their properties.

3.1. Brownian walkers

We begin with the case of Brownian motion (3) where we want to investigate the properties of the spatial distributions and compare our results with the 1D model. It has been discussed in [20] that in the case of Brownian walkers one can expect the emergence of 2D animal clusters with properties similar to those observed in 1D simulations. We therefore choose the 'baseline' movement parameters as $\sigma = 0.02$, $P = 0.6$ and $R = 1$ to make our 2D simulation consistent with the 1D model.

One example of the development of the spatial distribution over time is shown in Fig. 6. The formation of clusters is already seen at time $t = 100$, with no apparent difference between the distributions at times $t = 1000$ and $t = 10000$. This suggests that the system evolves to a steady spatial distribution as in the 1D model [20]. To investigate this further, we calculate the number of clusters and their population and spatial size using the definition of a cluster in Section 2.2. To determine the population and spatial size of the clusters we calculate the mean number of individuals in each cluster and also the mean area that each cluster covers for all clusters identified in the system at a particular time step. The evolution of those properties over time is shown in Fig. 7 up to $t = 1000$. Although the system never reaches a steady state in a strict sense due to fluctuations in the population and area of clusters, it is readily seen that the properties converge and do so in a timescale $t \approx 200$. Extending the simulation time up to $t = 20000$ shows that the quasi-steady state holds as no further changes are seen.

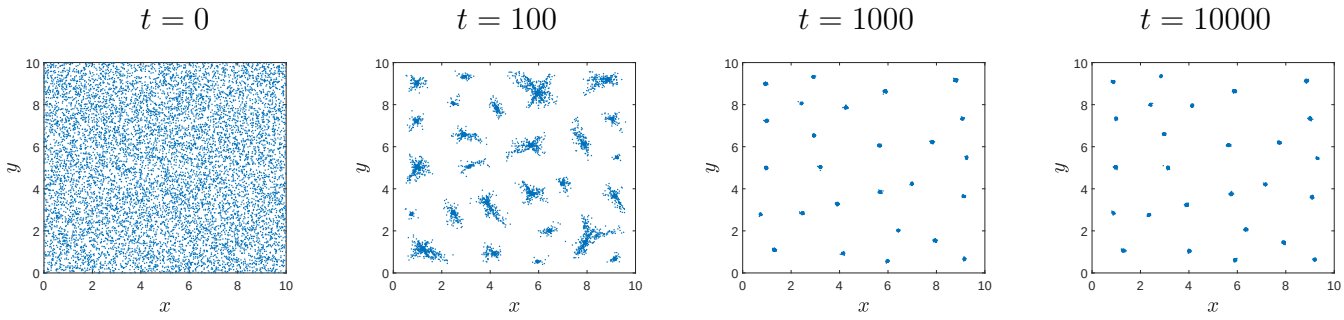

Figure 6: *The spatio-temporal dynamics emerging from a random-uniform initial distribution of a population of Brownian walkers at time* $t = 0$. *Movement parameters are* $P = 0.6$, $R = 1$ *and* $\sigma = 0.02$. *(a)* $t = 0$, *the initial distribution of the population; (b)* $t = 100$, *the formation of clusters already begin at small times; (c)* $t = 1000$ *and (d)* $t = 10000$, *clusters are 'temporally stable', as there is no visible change in the number of clusters and their shape over time.*

Stable formation of clusters is further confirmed by results in Fig. 8 where spatio-temporal dynamics are examined for a lower probability, $P = 0.2$, of directed movement. In this case, we expect the initial timescale of cluster formation to be longer when P is small, and this can be seen in Fig. 8, showing cluster properties over time $t = 20000$. The convergence of cluster properties now happens at approximately $t = 600$ and there are larger fluctuations in the mean cluster population. This is because individuals will be more likely to move in and out of clusters than for higher values of P.

Tables 1 and 2 show how the number of clusters, the mean cluster area and the number of free individuals, i.e. animals that are not within a cluster, depend on the parameters of

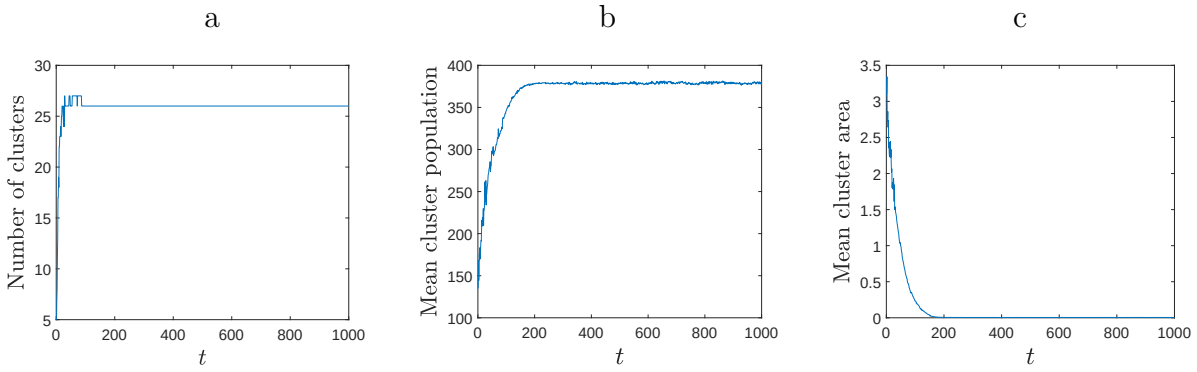

Figure 7: *An example of the development of clusters over time when the probability of directed movement is* $P = 0.6$. *The other parameters are* $R = 1$ *and* $\sigma = 0.02$. *The quantitative properties of the spatio-temporal dynamics are (a) the number of clusters, (b) the mean cluster population, and (c) the mean cluster area. The mean values of the cluster properties have been calculated from all the clusters that emerge in one simulation. The quantitative properties converge in a timescale* $t \approx 200$.

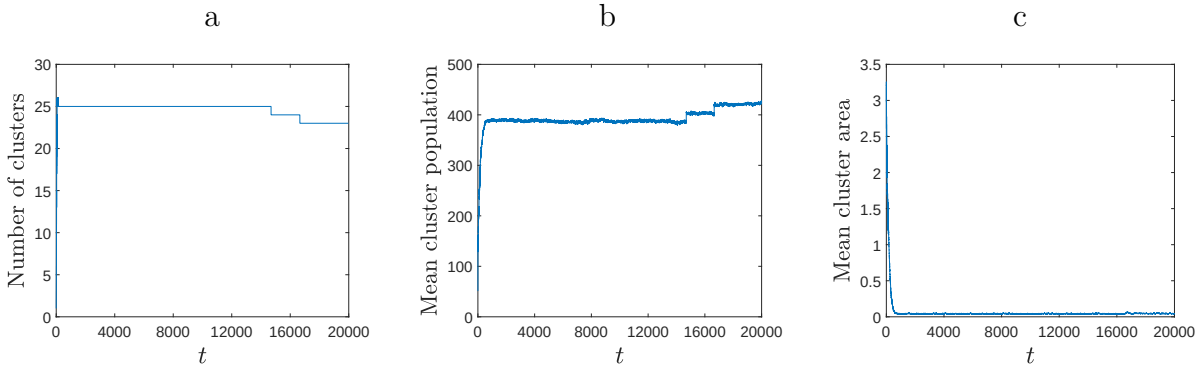

Figure 8: *An example of the development of clusters over time when the probability of directed movement is* $P = 0.2$. *The other parameters and the figure legend are the same as in Fig. 7. The quantitative properties converge in a timescale* $t \approx 600$.

directed movement. For each parameter set, 10 simulations are made up to $t = 10000$. We then record the number of clusters, the number of free individuals and the mean cluster area of all clusters in each simulation and take the mean of these numbers from all 10 simulations, giving the data in the tables.

Let us vary the probability P of directed movement. There are fewer individuals that will move further away from the centre of a cluster as P increases, because at each time step they have a high probability of moving directly to the centre. Therefore we expect that the animals will be clustered very densely and all animals will be contained within a cluster when P is large. This conclusion is confirmed by the results in Table 1. It is readily seen from the table that there is no significant trend in the number of clusters as P increases, but the cluster area and the number of free individuals decreases.

Table 2 shows the change in cluster properties when we vary the perception radius R. The significant trend when R is increased is that the number of clusters decreases with only

	$P = 0.1$	$P = 0.2$	$P = 0.3$	$P = 0.4$	$P = 0.5$	$P = 0.6$	$P = 0.7$	$P = 0.8$	$P = 0.9$
N_c	23.4	24.2	25.0	24.9	25.1	24.9	24.8	24.9	24.9
	(2.011)	(2.486)	(2.108)	(2.378)	(2.283)	(2.132)	(2.251)	(2.601)	(2.514)
$A_c \times 10^{-2}$	28.31	10.41	4.97	3.07	2.15	1.42	1.09	0.79	0.55
	(1.556)	(0.4148)	(0.2604)	(0.1695)	(0.07051)	(0.09906)	(0.04305)	(0.03562)	(0.03313)
n_f	499.4	222.2	138.1	111.2	80.3	52.6	52.4	58.3	40.1
	(68.96)	(42.50)	(51.99)	(45.41)	(26.29)	(26.55)	(26.82)	(23.17)	(26.51)

Table 1: *The mean and standard deviation of properties of clusters that form with different values of probability of directed movement P at $t = 10000$, $R = 1.0$, $\sigma = 0.02$; N_c is the mean number of clusters, A_c is the mean cluster area, n_f is the mean number of free individuals. The standard deviation for every mean value is shown in brackets below the mean. The values in the table are taken over* 10 *simulations.*

	$R = 1$	$R = 2$	$R = 2.523$	$R = 3$	$R = 4$	$R = 5$	$R = 100$
N_c	24.9	6.4	4.2	3.2	1	1	1
	(2.132)	(0.8433)	(0.6325)	(0.4216)	(0)	(0)	(0)
$A_c \times 10^{-2}$	1.42	2.30	2.80	2.82	3.26	4.10	3.24
	(0.09906)	(0.08758)	(0.1704)	(0.1499)	(0.4446)	(0.4149)	(0.5782)
n_f	52.6	24.9	12.9	15.2	1.8	1.9	6.9
	(26.55)	(20.99)	(9.927)	(13.92)	(5.007)	(4.434)	(8.293)

Table 2: *The mean and standard deviation of properties of clusters that form with different values of the perception radius R at $t = 10000$, $P = 0.6$, $\sigma = 0.02$. The legend is the same as in Table 1. The values in the table are taken over* 10 *simulations.*

individual clusters appearing when $R \geq 4$. This is because for large R each cluster will attract animals over a larger area. Since no two clusters can be within the perception radius of each other without coalescing, there will be space in the domain only for fewer clusters. We note that the value $R = 2.523$ in the table presents the case when the area within the perception radius covers 20% of the domain, i.e. the same proportion of the domain as when $R = 1$ in the 1D domain with $L = 10$ (see [20]). The mean number of clusters is $N_c = 4.2$ for $R = 2.523$ and is similar to the mean number of clusters in the 1D model with $R = 1$ which is given as $N_c = 4.56$. We also note that clusters (as we have defined them) are difficult to accurately identify until R is one order of magnitude greater than σ (see Fig. 9) and we therefore apply the requirement $R \gg \sigma$ when we proceed in our study so we can be confident that the cluster properties are correct.

Now that we understand how the density-dependent movement parameters P and R influence cluster formation we also want to check how the cluster properties are related to the basic characteristics of random movement, i.e. how they depend on the mean step size of Brownian walkers. Since we cannot directly control the mean step size in our computer simulations, we use the relationship (5) and vary the parameter σ in simulations instead. The results are shown in Table 3 where it is readily seen from the table that the choice of σ effects the number of clusters, the mean cluster area and the number of free individuals. As σ increases (and

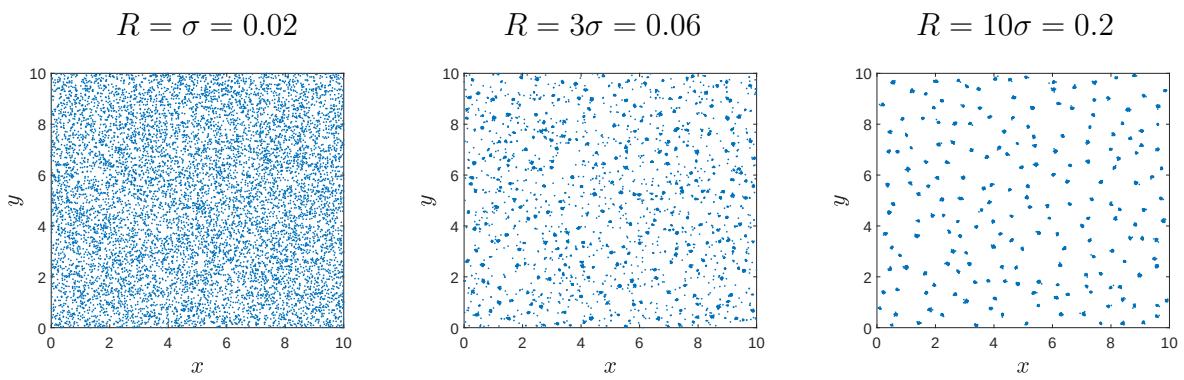

Figure 9: *Example distributions of a population of 10000 Brownian walkers at* $t = 10000$ *with small* R*. Other movement parameters are* $P = 0.6$ *and* $\sigma = 0.02$*.*

	$\sigma = 0.01$ $\mu_f = 0.008$	$\sigma = 0.02$ $\mu_f = 0.016$	$\sigma = 0.0332$ $\mu_f = 0.0265$	$\sigma = 0.04$ $\mu_f = 0.032$	$\sigma = 0.08$ $\mu_f = 0.064$	$\sigma = 0.2$ $\mu_f = 0.16$
N_c	25.8	24.9	24.6	24	19.1	11.5
	(1.81)	(2.13)	(1.71)	(1.16)	(1.46)	(0.850)
$A_c \times 10^{-2}$	0.355	1.42	3.64	5.18	19.2	78.2
	(0.0158)	(0.0991)	(0.199)	(0.227)	(0.914)	(5.66)
n_f	31.4	52.6	112	129	257	623
	(20.0)	(26.6)	(32.0)	(36.6)	(53.6)	(80.9)

Table 3: *The mean and standard deviation of properties of clusters that are formed by Brownian walkers with different values of* σ*. Given* σ*, the mean step size* μ_f *is defined according to (5). The legend is the same as in Table 1. The cluster properties are analysed at time* $t = 10000$*, other movement parameters are* $P = 0.6$ *and* $R = 1$*.*

the mean step size μ_f increases too), animals are more likely to take larger steps away from a cluster, leading to clusters with a larger area and in turn this means fewer clusters can exist in the domain as clusters must be a certain distance away from each other (see the discussion in appendix Appendix A). Taking a larger mean step size also means that animals are more likely to move entirely away from a cluster, leading to a higher number of free individuals. The change in properties is also visible in the example spatial distributions shown in Fig. 10.

We recall that the baseline case considered in our 1D model [20] is $R = 1$, $\sigma = 0.02$ and the mean number of clusters obtained in the 1D system with the above parameters is $N_c = 4.56$. Furthermore, we note that $\sigma = 0.0332$ in Table 3 corresponds to $\sigma = 0.02$ used in the 1D model via the relationship (5). Hence some comparison with the 1D model can be made if we change the perception radius from $R = 1$ to $R = 2.523$ as explained in our discussion of the perception radius above. The properties of spatial distributions obtained with $R = 1$ and $R = 2.523$ are presented in Table 4 where we can see that the mean number of clusters does not change and agrees well with our 1D results when we use the perception radius $R = 2.523$ in our simulations. Thus we conclude that the perception radius is a key parameter responsible for the number of clusters, while the choice of the mean step size makes an impact on the

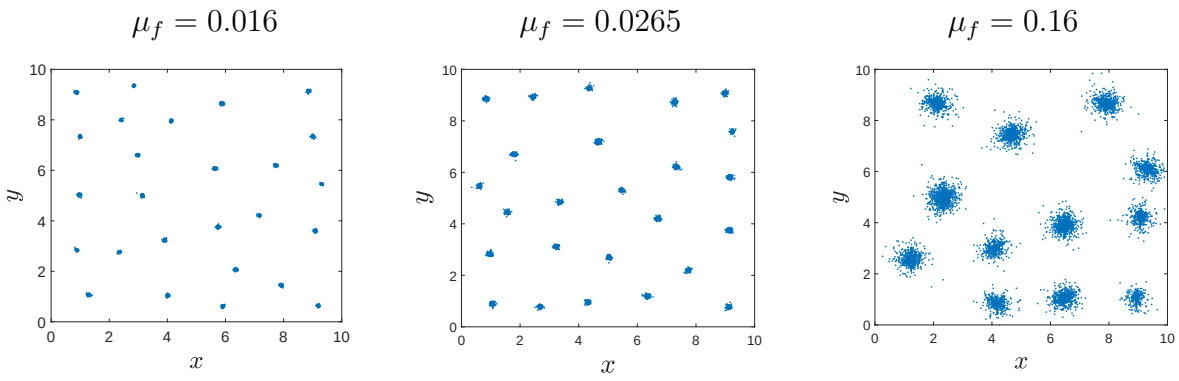

Figure 10: *Example distributions of a population of 10000 Brownian walkers at* $t = 10000$ *when* $\mu_f = 0.016$, $\mu_f = 0.0265$ *and* $\mu_f = 0.16$. *Other movement parameters are* $P = 0.6$ *and* $R = 1$.

mean cluster area and number of free individuals. Transition from $\sigma = 0.02$ to $\sigma = 0.0332$ while $R = 1$ results in a significant increase in the mean cluster area (see also an example distribution shown in Fig 10(b)).

	$\sigma = 0.02, R = 1$	$\sigma = 0.0332, R = 1$	$\sigma = 0.02, R = 2.523$	$\sigma = 0.0332, R = 2.523$
N_c	24.9	24.6	4.2	4.2
	(2.13)	(1.71)	(0.63)	(0.63)
$A_c \times 10^{-2}$	1.42	3.64	2.80	7.027
	(0.0991)	(0.199)	(0.1704)	(0.4569)
n_f	52.6	112	12.9	20.1
	(26.6)	(32.0)	(9.9)	(11.4)

Table 4: *The mean and standard deviation of properties of clusters that are formed by Brownian walkers with different values of* σ. *The legend is the same as in Table 1. The cluster properties are analysed at time* $t = 10000$ *at* $P = 0.6$.

Finally, we briefly investigate how cluster properties depend on the definition of the perception radius R. Let us introduce a 'decaying' perception range in the model when animals located closer to the individual are seen with a greater probability. The decaying perception radius can be modelled for each individual as follows. The distance d to all other animals is calculated and, for each other animal, the distance d is then compared to a random number r generated from a uniform distribution in the region $[R_0, R_1]$, where the radius $R_0 > 0$ and $R_1 > R_0$. If $r - d \geq 0$ then the animal is seen with probability 1 and influences the direction of movement. If $r - d < 0$, then the animal is not seen and has no influence on the direction of movement. Since $R_0 < r < R_1$, any distance $d \leq R_0$ will guarantee $r - d \geq 0$ and therefore the animal will definitely be seen and a distance $d > R_1$ will guarantee $r - d < 0$ and the animal will not be seen. Thus all animals within the radius of R_0 are seen, while only a fraction of the population located within the ring $R_0 < d < R_1$ is seen and no animals at the distance $d > R_1$ are seen.

The results obtained when we vary parameters R_0 and R_1 are presented in Table 5 (see also Fig. 11). From the results shown in the table, we conclude that introduction of the

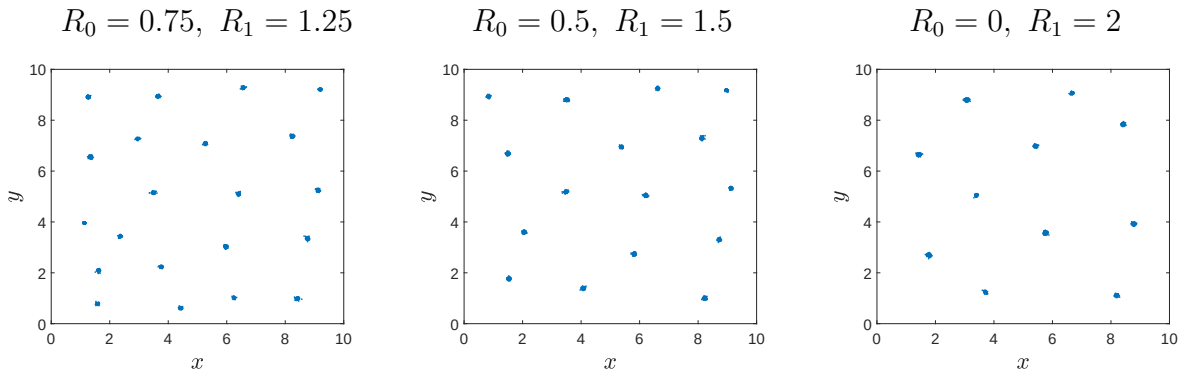

Figure 11: *Example distributions of a population of 10000 Brownian walkers at* $t = 10000$ *with a decaying perception radius. Other movement parameters are* $P = 0.6$ *and* $\sigma = 0.02$.

decaying perception range preserves cluster formation as clusters still form even when $R_0 = 0$. Meanwhile, the number of clusters decreases, as the size of the ring $R_0 < d < R_1$ is increased. This is similar to what happens when we use our standard definition of the perception radius and increase R (cf. Table 2). This is probably because, even though the probability of being 'seen' is small close to R_1, for a large population over a large number of time steps it will happen frequently enough for two clusters within the distance R_1 of each other to coalesce. Thus, our previous conclusion about the influence of the perception radius is confirmed as the average perception radius $(R_0 + R_1)/2$ can still be considered as a parameter of the density-dependent movement responsible for the number of clusters.

We conclude from the results in this section that the choice of the density-dependent movement parameters P and R influence the size and number of clusters respectively. The simulation results show a strong relationship between the number of clusters and the perception radius R. On the other hand, there is no significant relationship between the number of clusters and the probability of directed movement, P. Varying P in the model results in formation of less or more dense clusters where clusters with few or no free individuals are formed when P is sufficiently high. A similar effect can be observed when we decrease the

	$R = 1$	$R_0 = 0.75,\ R_1 = 1.25$	$R_0 = 0.5,\ R_1 = 1.5$	$R_0 = 0,\ R_1 = 2$
N_c	24.9	21.7	17.6	10.1
	(2.13)	(1.06)	(1.51)	(0.876)
$A_c \times 10^{-2}$	1.42	1.42	1.58	1.95
	(0.0991)	(0.0909)	(0.0927)	(0.133)
n_f	52.6	81.8	49	40.6
	(26.6)	(58.4)	(19.9)	(25.0)

Table 5: *The mean and standard deviation of properties of clusters that are formed by Brownian walkers with a decaying perception radius with different values of* R_0 *and* R_1 *at* $t = 10000$*, other movement parameters are* $P = 0.6$ *and* $R = 1$*. The legend is the same as in Table 1. The values in the table are taken over 10 simulations.*

mean step size, although the mean step size μ_f is not considered as an intrinsic parameter of density-dependent movement. Meanwhile, we want to emphasize the importance of the parameter P in our model. When $P = 0$, animals move independently of their conspecifics and introduction of the perception radius alone will not result in cluster formation (see also the discussion in section 4).

Also, given the dependence of cluster properties from the parameters of 2D density-dependent movement, we can confirm the assumption made in [20] that the formation of clusters in a 2D domain shares similar properties to the 1D model when Brownian walkers are considered. In particular, we see the same stable formation of clusters as shown in Figs. 7 and 8 and a similar number of clusters is formed when we use a 2D counterpart of the perception radius in the 1D model. Thus, a 1D model of density-dependent movement can be considered as a proxy for a study of 2D Brownian walkers to allow for significant computational savings and we can use conclusions made in [20] about the balance between parameters of random movement (i.e. the mean step size) and directed movement (i.e. the probability P and the perception radius R).

3.2. Non-Brownian walkers

In this section we consider non-Brownian motion simulated by a power law distribution (6). In order to make a sensible comparison between the results obtained for the dispersal kernel given by the normal distribution and those obtained for the power law, a certain condition of equivalence must be established. For distribution with a finite variance, one way for doing that is to equalize the variance of different probability distributions. However, this approach does not work in the most interesting case of fat-tailed distributions, i.e. Eq. (6) with $1 < \gamma \leq 3$, because the dispersal kernel (6) does not have a finite variance then. We therefore use a different approach [4], namely, we equalize the survival probabilities, i.e. the probabilities for the moving animal to remain within a given domain over a given interval. Let r_t be the radial distance of a given animal at a given time t, then the probability that at the next observation time $(t + 1)$ the animal will remain within a given distance δr of its previous location, i.e. $r_t - \delta r < r_{t+1} < r_t + \delta r$, is calculated as follows:

$$P\left(r_t - \delta r < r_{t+1} < r_t + \delta r\right) \;=\; \int_{-\delta r}^{\delta r} \rho(\xi) d\xi. \tag{10}$$

For the two probability distributions, see Eqs. (3) and (6), we obtain, respectively:

$$P\left(r_t - \delta r < r_{t+1} < r_t + \delta r\right) \;=\; \mathrm{erf}\left(\frac{\delta r}{\sqrt{2\sigma^2}}\right), \tag{11}$$

and

$$P\left(r_t - \delta r < r_{t+1} < r_t + \delta r\right) \;=\; 1 - \frac{k^{\gamma-1}}{(k + \delta r)^{\gamma-1}}. \tag{12}$$

Setting the the survival probability at a hypothetical value 0.9 and taking into account that $\mathrm{erf}^{-1}(0.9) = 1.16$, we solve Eqs. (11) and (12) for r and equate the results (since r is the same), thus arriving at the following relation between the parameters:

$$k \;=\; 1.16\sqrt{2\sigma^2}\left(10^{\frac{1}{\gamma-1}} - 1\right)^{-1}. \tag{13}$$

Therefore, for a given normal distribution with variance σ^2, parameter k of the 'equivalent' (in the sense explained above) power law distribution (6) is given by relation (13). We can also convert (13) to be in terms of the mean step size μ_f of the folded normal distribution as

$$k \;=\; 1.16\mu_f\sqrt{\pi}\left(10^{\frac{1}{\gamma-1}}-1\right)^{-1}. \tag{14}$$

When the exponent of the power law is $\gamma \leq 2$, then the distribution is heavy tailed and is used to simulate Levy flight. As we increase γ, the tail of the distribution becomes more like that of the normal distribution, and so we should expect the results to become similar to the results obtained for Brownian walkers (cf. the 1D problem [20]). Hence, for most simulations we set $\gamma = 2$, a commonly used parameter value for simulating Levy flight [51, 92, 93] but we will discuss the effect of changing γ further below. When analysing the clusters that form, we continue to use the definition in Section 2.2 with a grid of 20×20 bins and thresholds $b_u = 0.5\%$ of the total population N and $b_l = 0.25\%$ of the total population N. We also use the movement parameters $P = 0.6$, $R = 1$ and, following Eq. (13) with $\gamma = 2$ and $\sigma = 0.02$, we get $k = 0.0036$ to make our simulations compatible with Brownian walkers.

The development of the spatial distribution of non-Brownian walkers with the above choice of parameters is shown in Fig. 12. We see that areas of high population density form but they are not as clear and dense as the clusters formed by Brownian walkers. The clusters appear to form in the first 100 time steps and there is no obvious further congregation of the population between the distributions at $t = 500$ and $t = 20000$ from visual inspection although the number of clusters does appear to have changed.

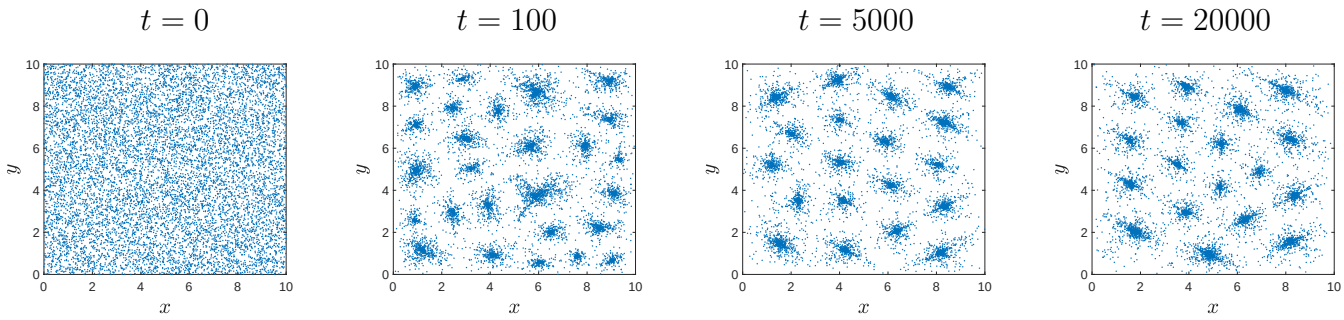

Figure 12: *The spatial distribution of a population emerging from a random-uniform initial distribution at time $t = 0$. The population moves according to a power law dispersal kernel (6) and the movement parameters are $P = 0.6$, $R = 1$, $\gamma = 2$, and $k = 0.0036$.*

The properties of the clusters formed by non-Brownian walkers are plotted in Fig. 13 for $P = 0.6$ and Fig. 14 for $P = 0.2$. When the probability of directed movement is sufficiently high, i.e. $P = 0.6$, the number of clusters drops several times in the first 4000 time steps and once more at $t \approx 8000$. The number of clusters then stays steady at $n = 18$ for the remaining time steps in the simulation. The mean cluster population shifts when the number of clusters changes (when two clusters merge, there will obviously be an increase in the mean cluster size) but is otherwise stable with small fluctuations as individuals move in and out of clusters. The mean cluster area stays relatively stable despite shifts in the number of clusters, suggesting

that the number of clusters and the cluster population have no impact on the spatial size of the cluster. When the probability of directed movement is $P = 0.2$, as shown in Fig. 14, the number of clusters over time is no longer fixed and instead fluctuates between 16 and 17 clusters, occasionally dropping to 15 and once to 14 clusters. The mean cluster population and area also fluctuate, much more wildly than for when $P = 0.6$ but there are no large shifts in either of those properties after the initial formation. The dynamics of a fluctuating number of clusters is similar to the dynamics seen in non-Brownian walkers in the 1D model where a similar analysis was done.

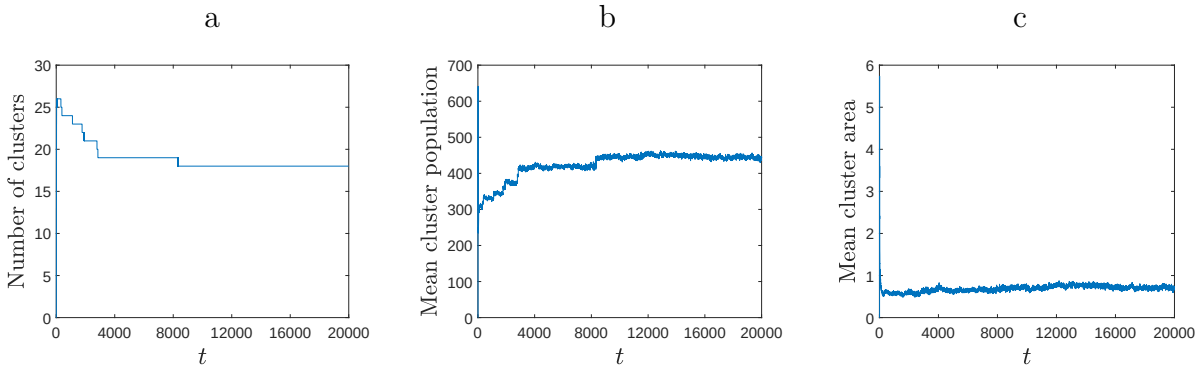

Figure 13: *The development of clusters over time. The population moves according to a power law dispersal kernel (6) and the movement parameters are $P = 0.6$, $R = 1$, $\gamma = 2$ and $k = 0.0036$. The quantitative properties of the spatio-temporal dynamics are (a) the number of clusters, (b) the mean cluster population , and (c) the mean cluster area. The system produces quasi-stable clusters with no strong fluctuations in the quantitative properties.*

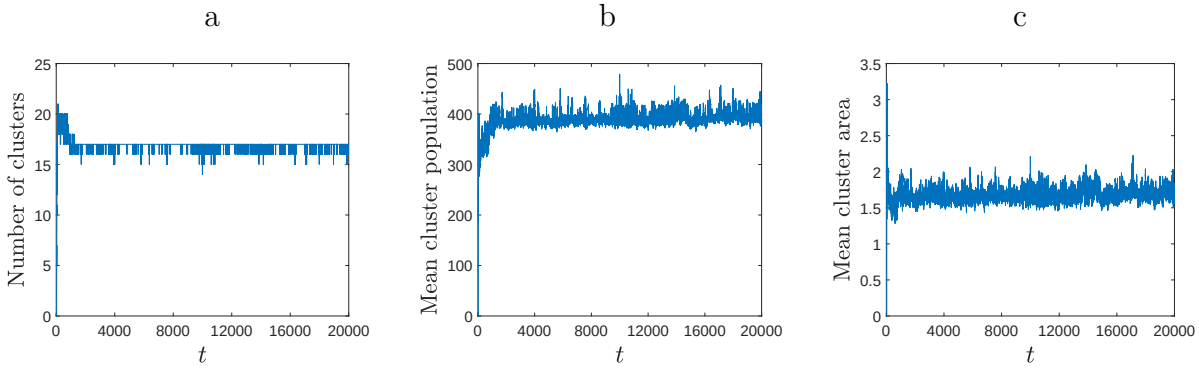

Figure 14: *The development of clusters over time. The population moves according to a power law dispersal kernel (6) and the movement parameters are $P = 0.2$, $R = 1$, $\gamma = 2$ and $k = 0.0036$. The quantitative properties of the spatio-temporal dynamics are (a) the number of clusters, (b) the mean cluster population , and (c) the mean cluster area. The number of clusters fluctuates with time resulting in fluctuations in the other quantitative properties.*

The results in Fig. 13 and 14 suggest that the stability or dynamism of the clusters is dependent on the probability P of directed movement. When $P = 0.6$ the system produces quasi-stable clusters, i.e. the number of clusters does not fluctuate although there may be

occasional changes in the number of clusters. When $P = 0.2$ however, we have a system where the number of clusters constantly fluctuates. We further investigate the dynamics of these clusters by calculating the rate of change of the number of clusters. Namely, we introduce a time interval consisting of ΔT time steps and a binary function $b(t)$, where $b(t) = 0$ if there is no change in the number of clusters over one time step, and $b(t) = 1$ if the number of clusters changed between $t - 1$ and t. The number of fluctuations $F(t)$ is then defined as

$$F(t) = \sum_{i=t-\Delta T}^{i=t} b(t_i). \tag{15}$$

The number of fluctuations $F(t)$ computed for $\Delta T = 100$ is shown in Fig. 15, where the value $F(t)$ at each time step is averaged over 10 simulations. It is seen from the figure that, after an initial time period, the number of fluctuations stays around 10 over time ΔT. In contrast, $F(t)$ calculated when $P = 0.6$ drops to close to 0 within 100 time steps and remains there for the rest of the simulation.

As discussed above, if the exponent of the power law, γ, is increased from $\gamma = 2$, the tail of the distribution decays quicker, becoming more like that of the normal distribution. We found in the 1D model that as γ is increased, the distributions that are produced become more similar to those produced by Brownian walkers. We expect that the same will hold true in the 2D model and we now examine the distributions that are produced with $2 \leq \gamma \leq 5$ and compare them with the population distribution of Brownian walkers. Table 7 shows that indeed, the properties of the clusters are more similar to the Gaussian dispersal kernel case when γ is higher. One notable difference is that when γ increases, so does the number of clusters (and standard deviation of the number of clusters). When γ is lower, there is a greater chance of individuals making larger steps. Intuitively, this means that clusters may have to be further apart otherwise they would merge together. The mean cluster area decreases, as γ increases, because the probability of an individual taking a large step away from the centre of the cluster is lower. We also see that, apart from $\gamma = 2$ when there are a large number of free individuals, the mean cluster population decreases as γ increases. This can be explained by the increase in the number of clusters since the whole population, which remains constant, is split between more clusters, resulting in smaller cluster populations. We note that when

	$R = 1$	$R = 2$	$R = 2.523$	$R = 3$	$R = 4$	$R = 5$	$R = 100$
N_c	20.7	4.5	3.8	1.9	1	1	1
	(1.45)	(0.527)	(0.422)	(0.738)	(0)	(0)	(0)
A_c	0.643	2.50	2.76	6.02	9.13	9.46	9.10
	(0.0457)	(0.359)	(0.318)	(2.75)	(0.541)	(0.595)	(0.611)
n_f	1998	1657	1639	1454	1286	1295	1321
	(62.3)	(109)	(63.2)	(136)	(50.4)	(45.6)	(51.9)

Table 6: *The mean and standard deviation of properties of clusters that are formed by non-Brownian walkers with different values of R at $t = 10000$, the other movement parameters are $P = 0.6$, $k = 0.00365$ and $\gamma = 2$. The values in the table are taken over 10 simulations.*

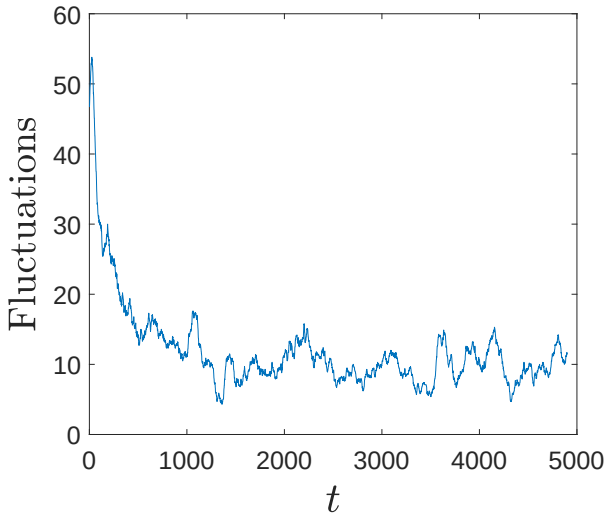

Figure 15: *The number of fluctuations in the number of clusters per* $\Delta T = 100$ *time steps averaged over 10 simulations. The populations in each simulation move according to a power law dispersal kernel (6) and the movement parameters are* $P = 0.2$, $R = 1$, $\gamma = 2$ *and* $k = 0.0036$.

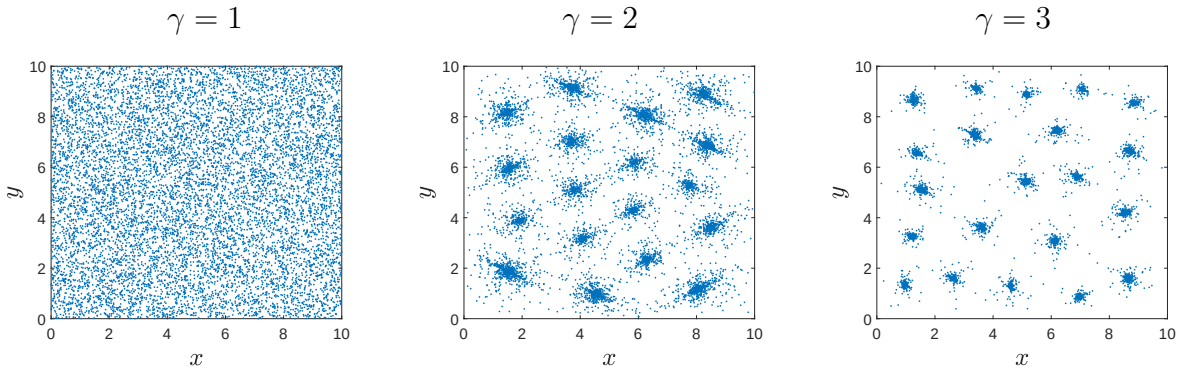

Figure 16: *The population distribution at* $t = 10000$ *of non-Brownian walkers using the power law distribution (6) to generate the step size with* $\gamma = 1,\ 2,\ 3$.

$\gamma = 1$, no clusters emerge in the population; cf. Fig. 16(a). This is due to the power law distribution (6) with $\gamma = 1$ meaning there is a high probability of an individual moving long distances within the domain. Therefore each individual will be consistently moving around the entire domain, never forming into clusters.

We now briefly discuss how basic characteristics of non-Brownian movement determined by (6) influence cluster formation. The investigation of this question is less straightforward than in the case of Brownian walkers (see section 3.1) as the power law distribution does not have a finite mean when $\gamma \leq 2$. Thus we pool together the movement step sizes made by all animals (i.e. $N = 10000$) in the population of non-Brownian walkers over 100 time steps and compute the 'mean step size' μ_n based on that information. Since the 'mean step size' μ_n obtained from direct computation depends on the parameter k in (6), we can vary it by varying k in in our computer simulations. Furthermore, as k is related to the parameter σ of the Brownian

Properties	$\gamma = 2$	$\gamma = 3$	$\gamma = 4$	$\gamma = 5$	Gaussian
N_c	20.7 (1.15)	20.1 (0.876)	22.7 (1.77)	23.3 (1.94)	24.9 (2.13)
A_c	0.643	0.248	0.118	0.0792	0.0153
	(4.57×10^{-2})	(2.11×10^{-2})	(1.2×10^{-2})	(8.75×10^{-3})	(1.05×10^{-3})
n_c	388 (22.3)	466 (22.8)	430 (36.1)	424 (39.1)	402 (36.9)

Table 7: *The mean and standard deviation of properties of clusters at* $t = 10000$ *that form in 10 simulations with different movement regimes,* N_c *is the mean number of clusters,* A_c *is the mean cluster area,* n_c *is the mean cluster population. The standard deviation for every mean value is shown in brackets. The parameters are* $R = 1$, $P = 0.6$, $k = 0.0036$, *and* $\sigma = 0.02$ *in the Gaussian case.*

motion by (13), a relationship between σ and μ_n can also be established. The results are shown in Table 8, where we take the same range of σ as in Table 3. Given the value σ, we find k from (13) and then determine μ_n from direct computation.

	$\sigma = 0.002$	$\sigma = 0.01$	$\sigma = 0.02$	$\sigma = 0.0332$	$\sigma = 0.2$
k	3.65×10^{-4}	1.82×10^{-3}	3.65×10^{-3}	6.05×10^{-3}	3.65×10^{-2}
μ_n	3.08×10^{-3}	0.0120	0.0218	0.0332	0.139

Table 8: *A comparison between* σ, k *and the 'mean step size'* μ_n *for non-Brownian walkers. Given the value* k, *the mean step size* μ_n *is calculated from the first 100 steps of* $N = 10000$ *animals in the simulated data.*

In Table 9 we calculate cluster properties when k is increased and therefore the 'mean step size' is increased according to the results in Table 8. It can be seen from the table that the same conclusion can be made as we had for Brownian walkers in section 3.1, i.e. the number of clusters N_c decreases as μ_n increases. It is worth noting, however, that cluster properties are different when the non-Brownian walkers are compared to Brownian walkers through the relationship between parameters in Table 8. For all values of σ we use in our simulations, the cluster size and number of free individuals is always larger for non-Brownian walkers (cf. Table 3). These results are also illustrated in Fig. 17 (cf. Fig. 10).

	$k = 3.65 \times 10^{-4}$	$k = 1.82 \times 10^{-3}$	$k = 3.65 \times 10^{-3}$	$k = 6.05 \times 10^{-3}$	$k = 3.65 \times 10^{-2}$
N_c	22.5	21.1	20.7	20.5	17.1
	(1.72)	(1.45)	(1.15)	(1.08)	(1.20)
$A_c \times 10^{-2}$	39.9	52.8	64.3	64.2	99.4
	(2.90)	(4.93)	(4.57)	(7.38)	(7.50)
n_f	1675	1839	1998	2089	2592
	(46.8)	(71.3)	(62.3)	(127)	(111)

Table 9: *The mean and standard deviation of properties of clusters that are formed by non-Brownian walkers with different values of* k *at* $t = 10000$, *the other movement parameters are* $P = 0.6$, $R = 1$ *and* $\gamma = 2$. *The values in the table are taken over* 10 *simulations.*

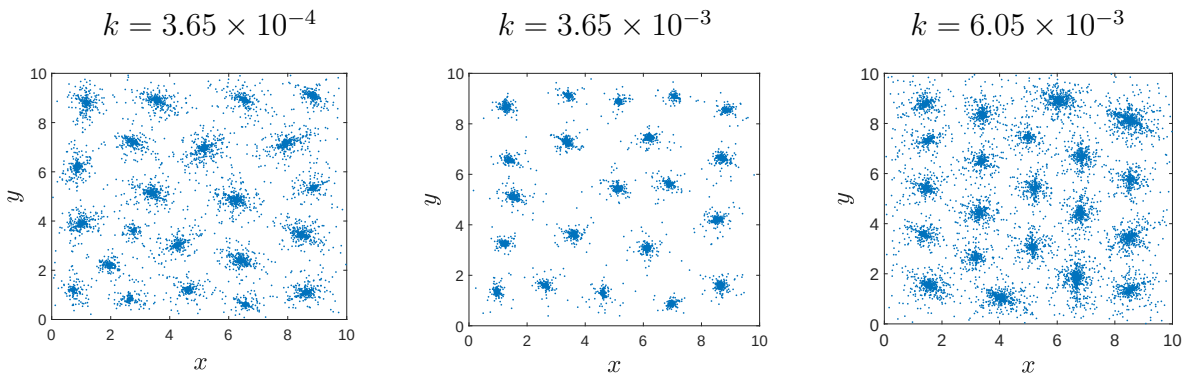

Figure 17: *Example distributions of a population of 10000 non-Brownian walkers at* $t = 10000$ *when* $k = 3.65 \times 10^{-4}$, $k = 3.65 \times 10^{-3}$ *and* $k = 6.05 \times 10^{-3}$. *Other movement parameters are* $P = 0.6$, $R = 1$ *and* $\gamma = 2$.

The simulations in this section show, as in the case of Brownian walkers, density-dependent movement by non-Brownian walkers results in the formation of clusters. However, like in the 1D case, the clusters formed by non-Brownian walkers are less dense than Brownian walkers and take a longer time to form. Also, the emergence of dynamic clusters, when the probability P of directed movement is low, has been revealed in the 2D case; see Fig. 14. Although the dynamics of fluctuating clusters was discussed in our previous paper [20], the dependence on the probability P of directed movement is a new result.

4. Comparison of Brownian and non-Brownian walkers

In this section we investigate the question of whether similar spatio-temporal dynamics of a population can emerge from Brownian and non-Brownian motion when different values of P are used. It has been shown in the previous sections that the probability of directed movement largely controls the size of the clusters that are produced; see Fig. 18 where the mean area of a cluster is shown to decrease as P increases. We have already established above and in our discussion of the 1D model [20] that the distributions produced by Brownian walkers are more dense than non-Brownian walkers. However, a numerical study reveals that there is an overlap where, for Brownian walkers with $P < 0.1$, there is a corresponding value of P for non-Brownian walkers that produces clusters with the same area.

Let us label the probabilities P of directed movement we use for Brownian and non-Brownian walkers as P_B and P_n respectively. To investigate further the similarities between clusters produced for Brownian walkers when $P_B < 0.1$ and non-Brownian walkers when $P_n > 0.1$, we compare the quantitative properties of clusters, i.e. the mean number of clusters, mean cluster population and mean area of clusters as well as the number of free individuals. We also measure the degree of aggregation in the population defined by the Morisita index [57]:

$$I_M = B \frac{\sum_{k=1}^{B} n_k(n_k - 1)}{N(N-1)} \tag{16}$$

where B is the number of bins, n_k is the number of animals in bin k and N is the total

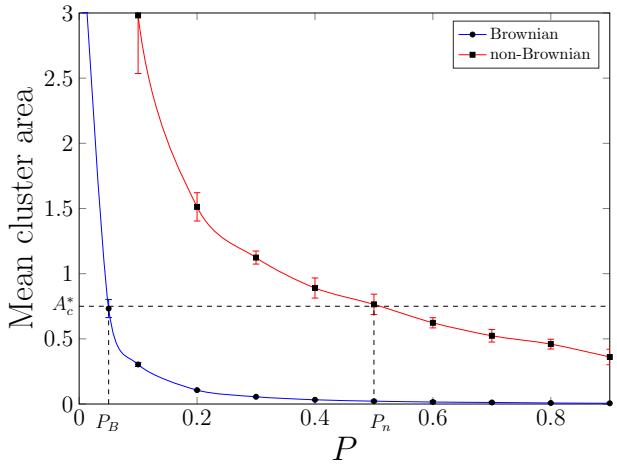

Figure 18: *The mean area of clusters of Brownian and non-Brownian walkers produced for the probability of directed movement* $P \in [0.01, 0.9]$. *The mean values of the cluster area in the graph are taken over* 10 *simulations for each value of* P *and the error bars show the standard deviation. For non-Brownian walkers, no clusters are formed when* $P < 0.05$. *The other movement parameters are* $R = 1$, $\sigma = 0.02$, $k = 0.0036$ *and* $\gamma = 2$. *Vertical dotted lines show two values of the probability* P *(i.e.* $P_B = 0.05$ *for Brownian motion and* $P_n = 0.5$ *for non-Brownian motion) that correspond to the same mean area of clusters* $A_c^* \approx 0.75$ *when simulation is done for Brownian and non-Brownian walkers respectively.*

population. The Morisita index provides a measure of how likely it is that two randomly selected individuals in a given distribution are found within the same bin compared to that of a random distribution. It has already been used in our study of 1D spatial distributions to quantify their heterogeneity. However, it is worth noting here that the Morisita index alone cannot be employed to compare various spatial distributions. Though it provides a measure of aggregation, the index (16) does not provide any information about the number of clusters or how they are distributed. Therefore it can only be used as an additional tool for comparing spatial distributions alongside the other quantitative properties of the clusters.

In Tables 10-11, we present the mean and standard deviation of features of the spatial distribution for Brownian walkers with certain values of P_B between 0.01 and 0.09 and non-Brownian walkers with P_n between 0.1 and 0.9. From close inspection of the data in the tables, we see that the properties of clusters are similar for Brownian and non-Brownian walkers when the probability of directed movement is approximately 10 times higher for non-Brownian walkers than for Brownian walkers, $P_n \sim 10P_B$. The exception to this relationship is when we compare clusters obtained for $P_B = 0.09$ and $P_n = 0.9$ as only the cluster population and area are similar, while the other properties start to diverge from each other as the probability increases.

Fig. 19 shows example distributions for simulations of Brownian and non-Brownian walkers at $t = 10000$ with various values of P_B and P_n. Visual inspection of these figures confirms that properties of clusters are similar when $P_n \sim 10P_B$ but only for $P_B \leq 0.05$, $P_n \leq 0.5$. As P increases the similarities of the cluster decrease and the spatial distributions are not as similar, as illustrated when $P_B = 0.08$ and $P_n = 0.8$.

Brownian walkers	$P_B = 0.01$	$P_B = 0.02$	$P_B = 0.05$	$P_B = 0.08$	$P_B = 0.09$
N_c	11.9	17.5	20.9	21.9	23.2
n_c	512.1	413.1	425.9	431.1	412.3
A_c	3.263	1.648	0.7324	0.4127	0.3538
n_f	3937	2803	1159	657.5	563.6
I_M	1.346	2.273	6.766	10.81	10.47
Non-Brownian walkers	$P_n = 0.1$	$P_n = 0.2$	$P_n = 0.5$	$P_n = 0.8$	$P_n = 0.9$
N_c	13.6	19.1	20.3	20.6	19.9
n_c	449.0	345.2	385.5	415.5	442.2
A_c	2.981	1.513	0.7643	0.4664	0.3716
n_f	3997	3437	2221	1508	1268
I_M	1.299	2.131	6.157	12.03	17.76

Table 10: *The mean of properties of clusters formed by Brownian and non-Brownian walkers at* $t = 10000$ *that form in 10 simulations with different movement regimes,* N_c *is the mean number of clusters,* n_c *is the mean cluster population,* A_c *is the mean cluster area,* n_f *is the mean number of free individuals,* I_M *is the Morisita index. Other parameters are* $R = 1$, $\gamma = 2$, $\sigma = 0.02$, *and* $k = 0.0036$.

Brownian walkers	$P_B = 0.01$	$P_B = 0.02$	$P_B = 0.05$	$P_B = 0.08$	$P_B = 0.09$
N_c	0.989	1.27	1.73	2.18	2.66
n_c	42.9	29.4	39.3	50.1	53.9
A_c	0.220	0.106	0.0600	0.0318	0.0198
n_f	318	162	138	115	84.5
I_M	0.0298	0.102	0.539	1.09	1.42
Non-Brownian walkers	$P_n = 0.1$	$P_n = 0.2$	$P_n = 0.5$	$P_n = 0.88$	$P_n = 0.9$
N_c	1.78	1.37	1.57	1.90	1.66
n_c	66.0	24.9	34.1	39.3	45.7
A_c	0.490	0.124	0.0705	0.0481	0.0499
n_f	190	209	116	75.8	118
I_M	0.0171	0.0449	0.450	1.56	5.86

Table 11: *The standard deviation of properties of clusters formed by Brownian and non-Brownian walkers at* $t = 10000$ *that form in 10 simulations with different movement regimes. Other parameters are* $R = 1$, $\gamma = 2$, $\sigma = 0.02$, *and* $k = 0.0036$. *The legend is the same as in Table 10.*

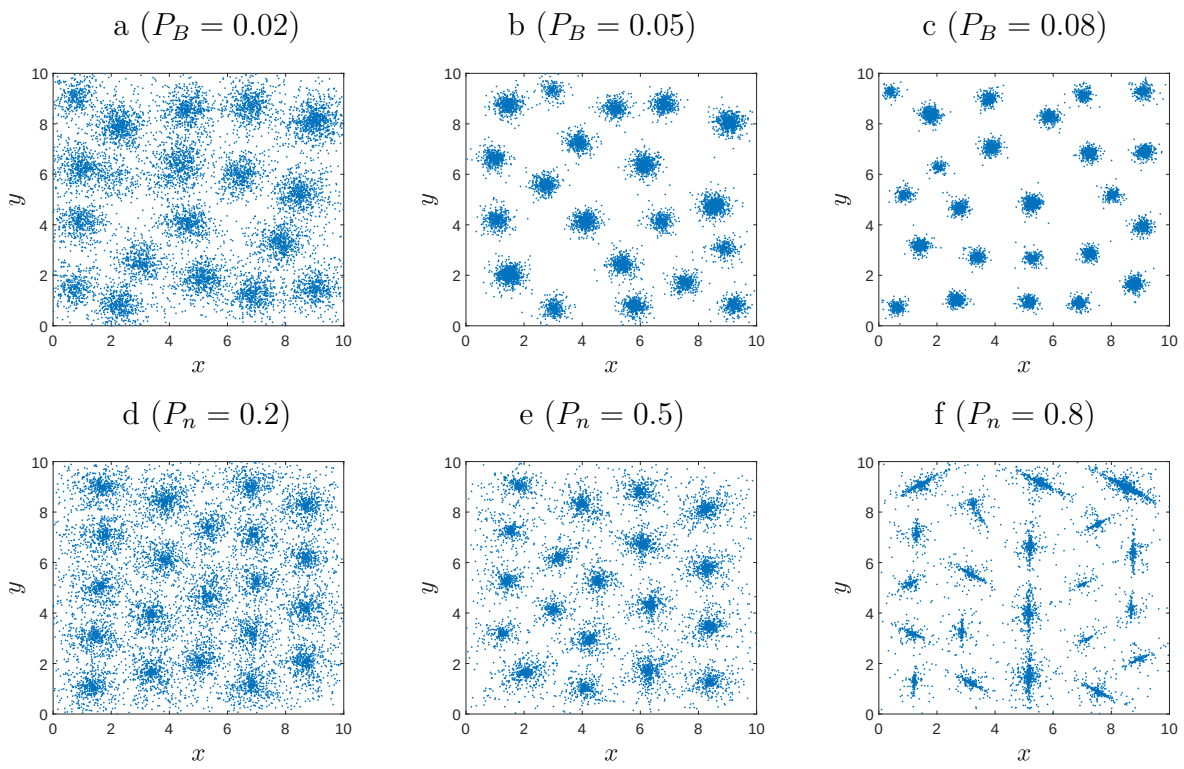

Figure 19: *Example distributions of Brownian walkers (top) and non-Brownian walkers (bottom) at* $t = 10000$ *with varying probabilities of directed movement. Probabilities* P_B *and* P_n *are shown in brackets for Brownian and non-Brownian walkers respectively. The other movement parameters are* $R = 1$, $\sigma = 0.02$, $k = 0.0036$ *and* $\gamma = 2$.

One result of directed movement in the 2D model is that for large P the shape of clusters becomes 'stretched'. One example of stretched clusters can be seen in Fig. 19f when $P_n = 0.8$ showing the distribution formed by non-Brownian walkers. To measure the difference between the shapes of a 'stretched' cluster of Fig. 19f and a 'uniform disk' cluster of Fig. 19c, we analyse the distribution of angles from the centre of the cluster in each spatial distribution of animals in a cluster. Namely, the median position $\mathbf{r}_m$ of all animals within the cluster is calculated for spatial distributions in Fig. 19c and Fig. 19f. We then find the angle of each animal to the point $\mathbf{r}_m$ and then re-orientate each cluster in the spatial distribution so that the peak angles are at $\pm\pi/2$. This allows us to use data from all the clusters in the distribution to generate a histogram of angle frequencies as shown in Fig. 20 (a,c). The slope from the peak at $\pi/2$ can then be fitted with a power law distribution as shown in Fig. 20(b,c). From examining the figures and fitting the slope from $\pi/2$ to π we conclude that the clusters produced by Brownian and non-Brownian walkers have a very different shape indeed, despite having similar cluster properties.

Formation of 'stretched' clusters is in part due to formulation of our model where we use splitting the area inside an animals perception radius into segments. We believe this rule makes sense biologically as an animal is unlikely to move in a direction which it perceives to be the mean position of its cospecifics rather than a direction which it perceives to have the

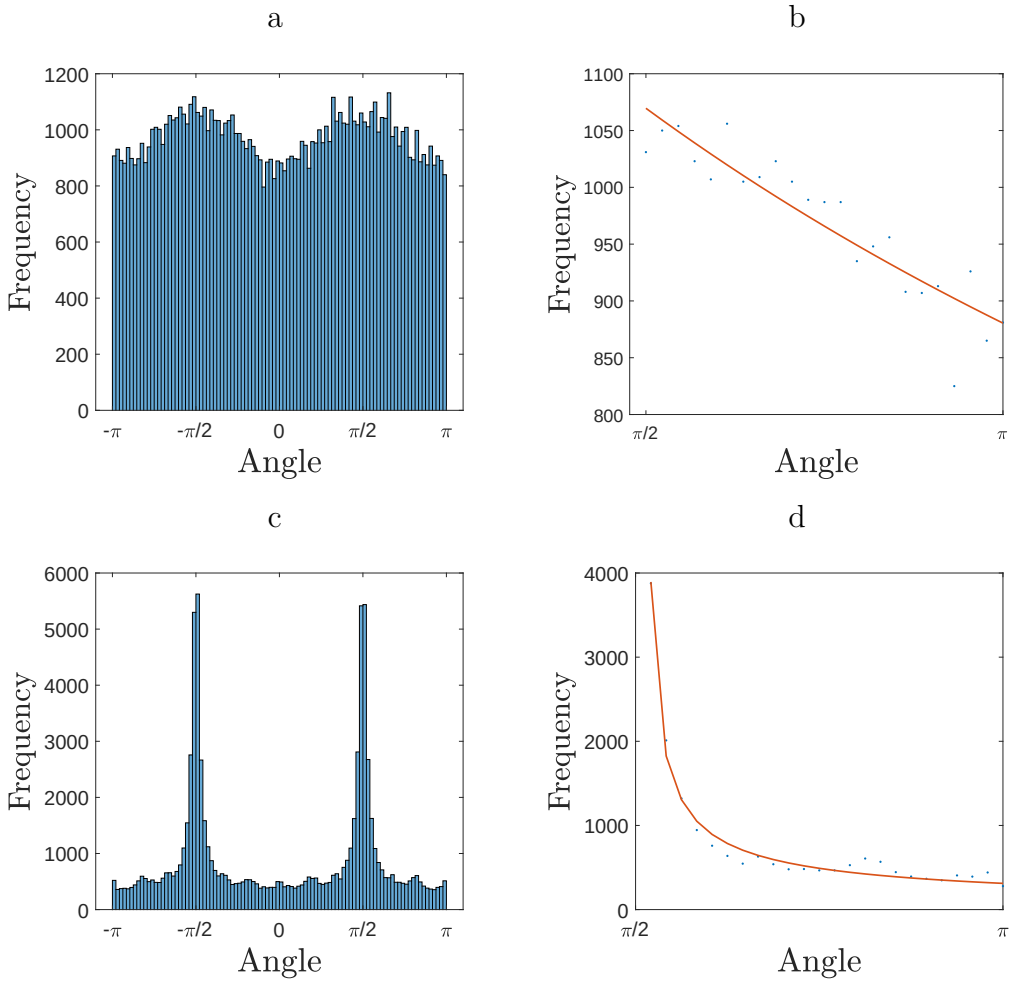

Figure 20: *(a) The distribution of angles between animals in a cluster and the centre of the cluster for all clusters shown in Fig. 19 produced by Brownian walkers when* $P_B = 0.08$ *(a,b) and non-Brownian walkers when* $P_n = 0.8$ *(c,d). The distribution between* $\pi/2$ *and* π *fitted with a power law distribution is (b)* $6941/(6.558+\theta)^{0.989}$ *with* $r^2 = 0.83$*, and (d)* $404/(-0.037+\theta)^{0.632}$ *with* $r^2 = 0.98$*.*

highest density. The use of segments narrows down the direction an animal will decide to move to a region that contains the highest density. We acknowledge however, that there may be other methods of modelling density dependent movement that do not result in stretched clusters and further study is required to understand the phenomenon.

We have seen above that the appearance of dynamic clusters, i.e. spatio-temporal dynamics where the number of clusters fluctuates over time, is dependent on the probability P_n of directed movement in non-Brownian walkers. Meanwhile, it immediately follows from comparison of Figs. 13(a) and 14(a) that dynamic clusters are not a feature that presents in the system of non-Brownian walkers for all values of P_n. For example, dynamic clusters appear when $P_n = 0.2$ in Fig. 14(a), yet there are no dynamic clusters when $P_n = 0.6$ in Fig. 13(a). Furthermore, if we suppose that Brownian walkers with the $P_B = 0.02$ produce similar clusters to non-Brownian walkers with the 'counterpart' probability $P_n = 0.2$, then we might expect those clusters to be dynamic when the spatio-temporal dynamics of Brownian walkers is con-

sidered. However, as Fig. 21(a) shows, the clusters appear to be stable with only a shift in the number of clusters happening at $t \approx 3500$. This is obviously different to the dynamics of non-Brownian walkers when $P_n = 0.2$ on the same timescale.

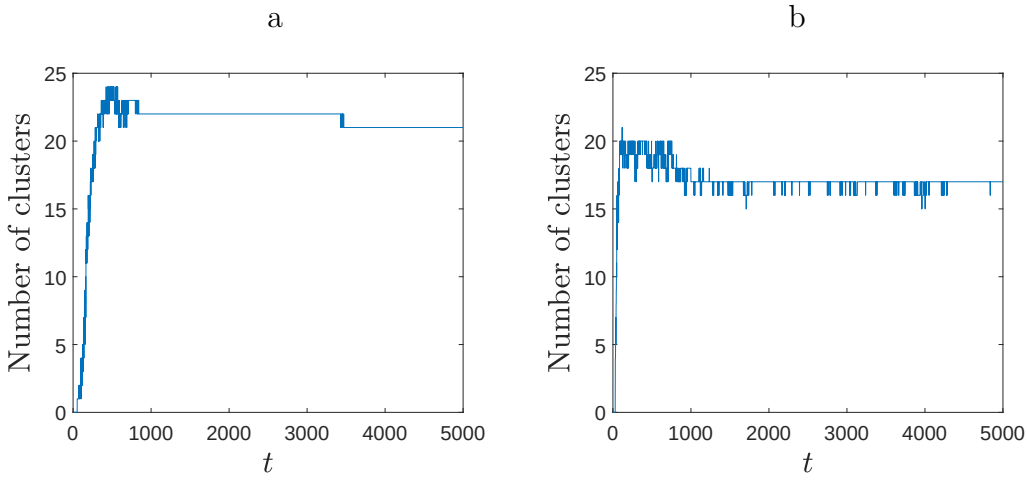

Figure 21: *The number of clusters over time for (a) Brownian walkers with $P_B = 0.02$ and (b) non-Brownian walkers with $P_n = 0.2$. The other movement parameters are $R = 1$, $\sigma = 0.02$, $k = 0.0036$ and $\gamma = 2$.*

We can therefore conclude that for certain probabilities of directed movement, the distributions produced by Brownian and non-Brownian walkers can appear similar. This only holds for $P_B < 0.05$ for Brownian walkers for some corresponding P_n for non-Brownian walkers. While some cluster properties remain similar, the shape of clusters and the cluster stability are not. Moreover, as P_B increases, other properties such as the number of free individuals produced by each movement type diverge and when $P_B > 0.1$ there is no corresponding P_n that will produce a similar distribution. Due to the difference in cluster stability, we have the important result that while the spatial distributions of Brownian walkers and non-Brownian walkers can be indistinguishable when considering certain cluster properties, the spatio-temporal dynamics are still different.

5. Discussion and conclusions

Spatial aggregation is important in many areas of ecological research including population dynamics [58, 72, 44], nature conservation and renewable resource management [18, 99, 100], agriculture and forestry [1, 42, 80, 84, 95], and monitoring and pest control [67, 70, 73]. Whilst understanding of this phenomenon has significantly improved over the last decades [47, 52, 55, 65], the effect of many relevant factors on the ecological pattern formation, in particular the role of the movement of individuals, remains poorly understood in spite of it arguably being a key factor in spatial ecology [9, 61].

In our previous paper [20], we developed a 1D model of a population where individuals move with density-dependence. Our aim was to relate the problem of understanding of population spatial patterning to another major focus in ecology, namely, to the effect of different individual

movement patterns [76, 88, 93]. We therefore considered the spatial dynamics of a population where animals perform either Brownian or non-Brownian density-dependent motion. In this paper, the model of density-dependent movement has been extended to 2D spatial domains. We have designed the formulation of the process of directed movement in a 2D domain: while the size of a random jump is consistent between the 1D and 2D cases, the introduction of an angle of movement in the 2D model influences how directed movement works. Namely, when the probability of directed movement is $P = 0.5$ in the 1D model, there is unbiased random movement as there is an equal chance of an animal moving towards the area of higher density. In the 2D model, having the probability $P = 0.5$ does not result in unbiased random movement as the animal will move directly towards the area of highest density in 50% of time steps and at any other angle the other 50%. Therefore, it is only the value $P = 0$ that produces unbiased random movement in the 2D model. This makes it difficult to compare the results of the 1D and 2D models when changing P directly. Instead, in this paper we have shown how the spatial distributions are dependent on P throughout the range of $P \in (0, 1)$. We have also investigated how the spatial distributions depend on the perception radius R - another parameter required to formulate rules of density-dependent movement in the model.

5.1. Brownian walkers

We concluded in our study in [20] that the formation of clusters in a population of Brownian walkers would be similar in 1D*and*2D models. Indeed, in the case of Brownian walkers and assuming that the environment is isotropic, the 'full' 2D movement splits to a product of two 1D movements for x and for y, i.e. $\rho(\Delta\mathbf{r}) = \rho(\Delta x)\,\rho(\Delta y)$ where $\Delta\mathbf{r}$ is the movement step along the 2D path, $(\Delta\mathbf{r})^2 = (\Delta x)^2 + (\Delta y)^2$, and each of $\rho(\Delta x)$ and $\rho(\Delta y)$ is given by (3). In this study we have confirmed that density-dependent movement in 2D spatial domains results in the formation of animal clusters and, exploring the changes in cluster properties as the parameters change, we have found that the relationship between parameters and the distribution is the same in 1D and 2D problems. The number of clusters formed in a 2D domain is random although within a range that is dependent on the movement parameters, particularly the perception radius R. When we set the area within the perception radius to be the same proportion of the domain in the 2D model as the 1D model, the mean number of clusters in 2D is 4.2, while in 1D the mean number of clusters is 4.56. In both studies, increasing the perception radius led to fewer clusters. In both 1D and 2D cases, given that P is sufficiently high then dense clusters were formed with few or no free individuals. Only when P was very close to the value where the movement becomes unbiased (i.e. $P \approx 0.52$ in 1D, $P \approx 0.01$ in 2D) did the random movement not result in clusters. When P was such that clusters did form they were always stable and although there were occasional changes in the number of clusters, Brownian walkers never produced dynamic, rapidly fluctuating clusters.

5.2. Non-Brownian walkers

The formation of clusters by a population of non-Brownian walkers in the 2D model was less predictable having studied the results in 1D spatial domains. We found that indeed, clusters were formed in the population of non-Browian walkers. Similarly to the 1D model, for the

same parameter choice the properties of 2D clusters differ significantly between populations of Brownian and non-Brownian walkers. The non-Brownian walkers produce fewer clusters that are less dense and there are many more free individuals in the domain in comparison to Brownian walkers with equivalent movement parameters.

It has been revealed in our 2D study that there are similarities between properties of clusters formed by Brownian walkers with $P < 0.1$ and non-Brownian walkers with a value of P approximately 10 times larger. This conclusion, however, does not hold for the stability of clusters as Brownian walkers do not produce dynamic clusters for any P. Thus, the analysis of spatial distributions alone may not be sufficient to conclude about the movement type: the spatial distributions of Brownian walkers and non-Brownian walkers can be indistinguishable when considering certain cluster properties but the spatio-temporal dynamics are still different.

Another new feature of the 2D problem is that the clusters of non-Brownian walkers are dynamic but only when P is sufficiently low. In our study of the 1D model, we concluded that non-Brownian walkers produced dynamic clusters while Brownian walkers produced stable clusters. However, by analysing the dynamics with varying values of P in the 2D model, we have now found that 2D clusters produced by non-Brownian walkers are not always dynamic.

5.3. Summary of cluster dynamics in the 2D model

We have shown that the probability of directed movement, P, has a significant effect on the properties of clusters that arise from density dependent movement of both Brownian and non-Brownian walkers. When $P = 0$, animals move independently of their conspecifics and therefore the system will preserve an initial statistically uniform distribution for Brownian and non-Brownian walkers. As P increases, at some point the system will shift so that a distribution is produced that contains clusters. This will occur at a different value of P depending on the movement type. For non-Brownian walkers, clusters will begin to form at $P \approx 0.05$ but for Brownian walkers this probability value will be much lower, $P \approx 0.01$.

When clusters are formed in a population of Brownian walkers, they are largely stable over time (apart from occasional shifts when clusters merge), as shown in Fig. 21(a) with $P = 0.02$. However, for clusters that are formed in a population of non-Brownian walkers with a low value of P, the number of clusters is dynamic, as shown in Fig. 21(b) with $P = 0.2$. At some point between $P = 0.2$ and $P = 0.6$ another shift occurs for non-Brownian walkers and the clusters that are produced become stable, as seen in Fig. 13(a).

It is difficult to study the exact points of transition when increasing P as it would involve numerous simulations. We therefore cannot say for certain whether the shifts from the 'no clusters' region in P to 'dynamic clusters' to 'stable clusters' happen suddenly, neither we can determine the length of the transition state between the two. However, we can approximately find the regions of different dynamics by running multiple simulations with varying P. Fig. 22 shows the number of fluctuations in the non-Brownian walkers case when P increases with the increment 0.025. Between $P = 0.05$ and $P = 0.175$ we have a very high rate of fluctuations that starts decreasing as P increases. For $P = 0.2$ to $P = 0.275$ there are still a small number of fluctuations which then suddenly drops to almost no fluctuations happening at $P = 0.3$ and above. The results shown in the figure do suggest a sharp shift in the dynamics, first from

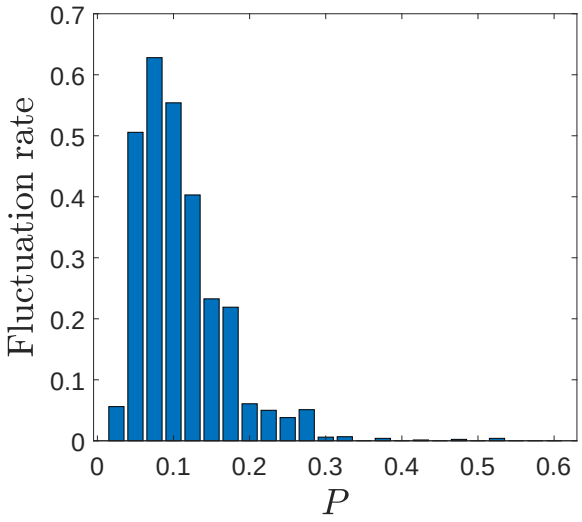

Figure 22: *The rate of fluctuations in the number of clusters between* $t = 4000$ *and* $t = 5000$ *in a population of non-Brownian walkers when* P *increases from* $P = 0.025$ *to* $P = 0.6$ *with the increment* $\Delta P = 0.025$*. The populations in each simulation move according to a power law dispersal kernel (6) and the movement parameters are* $R = 1$*,* $\gamma = 2$ *and* $k = 0.0036$*. The frequencies are averaged over three simulations for each value of* P*.*

no clusters to highly dynamic clusters at $P = 0.05$ which then has a slow shift to moderately dynamic clusters at $P = 0.2$ and another sharp shift to stable clusters at $P = 0.3$.

As discussed above, the number of clusters is dependent on our definition and choice of threshold parameters and bin size. We chose parameters so that the properties of clusters would not be sensitive to small changes in those parameters. However at transitions between dynamics of the distributions the choice of parameters may have a greater effect. Further to this, we have not formally defined what we mean by stable and dynamic clusters. It is clear that Fig. 21(b) shows dynamic clusters but if the number of transitions was decreased there must be a threshold at which point we would consider the system to no longer be showing dynamic clusters and this issue requires further investigation.

Our plans for future work will be to utilise the generic model in a particular problem - that of estimating the spatial distribution of a population that undergoes density-dependent movement from a grid of animal traps. Specifically we will be fitting our parameters to field data from the grey field slug *Deroceras reticulatum* who develop into patchy spatial distributions [24, 70]. Understanding of the mechanisms underpinning the observed spatial and temporal stability of slug patches through combination of numerical simulation and analysis of field data will constitute a topic of future research.

Acknowledgements

J.R.E. acknowledges support in the form of a Research Associateship from the School of Mathematics, University of Birmingham. Helpful and thought-provoking comments made by two anonymous referees are gratefully acknowledged.

References

[1] Alexander, C.J., Holland, J.M., Winder, L., Woolley, C., Perry, J.N., 2005. Performance of sampling strategies in the presence of known spatial patterns. Ann Appl Biol 146, 361–370.

[2] Archard, G.A., Bohan, D.A., Hughes, L., Wiltshire, C.W., 2004. Spatial sampling to detect slug abundance in an arable field. Ann Appl Biol 145, 165–173.

[3] Aurenhammer, F., 1991. Voronoi diagrams—a survey of a fundamental geometric data structure. ACM Comput Surv 23, 345–405.

[4] Bearup, D., Benefer, C.M., Petrovskii, S.V., Blackshaw, R.P., 2016. Revisiting Brownian motion as a description of animal movement: a comparison to experimental movement data. Methods Ecol Evol 7, 1525–1537.

[5] Beyer, K., Goldstein, J., Ramakrishnan, R., Shaft, U., 1999. When is "nearest neighbor" meaningful?, in: International conference on database theory, Springer. pp. 217–235.

[6] Bohan, D.A., Glen, D.M., Wiltshire, C.W., Hughes, L., 2000. Parametric intensity and the spatial arrangement of the terrestrial mollusc herbivores *Deroceras reticulatum* and *Arion intermedius*. J Anim Ecol 69, 1031–1046.

[7] Brattstrom, B.H., 1962. Thermal control of aggregation behavior in tadpoles. Herpetologica 18, 38–46.

[8] Broly, P., Mullier, R., Deneubourg, J.L., Devigne, C., 2012. Aggregation in woodlice: social interaction and density effects. ZooKeys , 133.

[9] Bullock, J.M., Kenward, R.E., Hails, R.S., 2002. Dispersal Ecology: 42nd symposium of the British ecological society. Cambridge University Press.

[10] Buss, L., Jackson, J., 1979. Competitive networks: nontransitive competitive relationships in cryptic coral reef environments. Am Nat 113, 223–234.

[11] Byers, J.A., 2000. Wind-aided dispersal of simulated bark beetles flying through forests. Ecol Model 125, 231–243.

[12] Cao, R., Cuevas, A., Manteiga, W.G., 1994. A comparative study of several smoothing methods in density estimation. Comput Stat Data An 17, 153–176.

[13] Carrascau, L.M., Alonso, J.C., Alonso, J.A., 1990. Aggregation size and foraging behaviour of white storks *(Ciconia cinconia)* during the breeding season. Ardea 78, 399–404.

[14] Clark, P.J., Evans, F.C., 1954. Distance to nearest neighbor as a measure of spatial relationships in populations. Ecology 35, 445–453.

[15] Codling, E.A., Plank, M.J., Benhamou, S., 2008. Random walk models in biology. J R Soc Interface 5, 813–834.

[16] Cowie, R., Krebs, J., 1979. Optimal foraging in patchy environments. population dynamics, in: 20th Symposium of British Ecological Society (Ed by RM Anderson, BD Turner & LR Taylor), pp. 183–205.

[17] Danchin, E., Wagner, R.H., 1997. The evolution of coloniality: the emergence of new perspectives. Trends Ecol Evol 12, 342–347.

[18] Dunning, J.B., Stewart, D.J., Danielson, B.J., Noon, B.R., Root, T.L., Lamberson, R.H., Stevens, E.E., 1995. Spatially explicit population models: current forms and future uses. Ecol Appl 5, 3–11.

[19] Edelsbrunner, H., Kirkpatrick, D., Seidel, R., 1983. On the shape of a set of points in the plane. IEEE T Inform Theory 29, 551–559.

[20] Ellis, J., Petrovskaya, N., Petrovskii, S., 2019. Effect of density-dependent individual movement on emerging spatial population distribution: Brownian motion vs Levy flights. J Theor Biol 464, 159–178.

[21] Ellis, J.R., 2020. Github repository. `https://github.com/John-R-Ellis/density-dependent-IBM`.

[22] Ellis, P.E., 1959. Learning and social aggregation in locust hoppers. Anim Behav 7, 91–106.

[23] Fisher, J., 1954. Evolution and bird sociality. Evolution as a Process , 71–83.

[24] Forbes, E., Back, M., Brooks, A., Petrovskaya, N., Petrovskii, S., Pope, T., Walters, K.F.A., 2017. Sustainable management of slugs in commercial fields: Assessing the potential for targeting control measures. Asp Appl Biol 134, 89–96.

[25] Fortin, M.J., Dale, M.R., Ver Hoef, J.M., 2002. Spatial analysis in ecology. Wiley StatsRef: Statistics Reference Online 4, 2051–2058.

[26] Gilinsky, E., 1984. The role of fish predation and spatial heterogeneity in determining benthic community structure. Ecology 65, 455–468.

[27] Graves, B.M., Duvall, D., 1987. An experimental study of aggregation and thermoregulation in prairie rattlesnakes *(Crotalus viridis viridis)*. Herpetologica 43, 259–264.

[28] Grimm, V., 1994. Mathematical models and understanding in ecology. Ecol Model 75, 641–651.

[29] Grimm, V., Railsback, S.F., 2013. Individual-based modeling and ecology. volume 8. Princeton university press.

[30] Grünbaum, D., 2012. The logic of ecological patchiness. Interface Focus 2, 150–155.

[31] Grünbaum, D., Okubo, A., 1994. Modelling social animal aggregations, in: Frontiers in mathematical biology. Springer, pp. 296–325.

[32] Gueron, S., Levin, S.A., Rubenstein, D.I., 1996. The dynamics of herds: From individuals to aggregations. J Theor Biol 182, 85–98 .

[33] Gurevitch, J., 1986. Competition and the local distribution of the grass *Stipa neomexicana*. Ecology 67, 46–57.

[34] Hassell, M.P., May, R.M., 1973. Stability in insect host-parasite models. J Anim Ecol 42, 693–726.

[35] Heinsalu, E., Hernández-García, E., López, C., 2010. Spatial clustering of interacting bugs: Lévy flights versus Gaussian jumps. EPL-Europhys Lett 92, 40011.

[36] Henne, D.C., Thinakaran, J., 2020. Spatially explicit changes in potato psyllid (hemiptera: Triozidae) populations in three south texas potato fields. J Econ Entomol 113, 988–1000.

[37] Hutchinson, G.E., 1953. The concept of pattern in ecology. P Acad Nat Sci Phila 105, 1–12.

[38] Jeltsch, F., Moloney, K., Milton, S.J., 1999. Detecting process from snapshot pattern: lessons from tree spacing in the southern Kalahari. Oikos 85, 451–466.

[39] Jopp, F., Reuter, H., 2005. Dispersal of carabid beetles—emergence of distribution patterns. Ecol Model 186, 389–405.

[40] Kareiva, P., 1983. Local movement in herbivorous insects: applying a passive diffusion model to mark-recapture field experiments. Oecologia 57, 322–327.

[41] Keller, E.F., Segel, L.A., 1970. Initiation of slime mold aggregation viewed as an instability. J Theor Biol 26, 399–415.

[42] Kelly, D., 1994. The evolutionary ecology of mast seeding. Trends Ecol Evol 9, 465–470.

[43] Kolokolnikov, T., Carrillo, J.A., Bertozzi, A., Fetecau, R., Lewis, M., 2013. Emergent behaviour in multi-particle systems with non-local interactions. Physica D 260, 1–4.

[44] Van de Koppel, J., Gascoigne, J.C., Theraulaz, G., Rietkerk, M., Mooij, W.M., Herman, P.M., 2008. Experimental evidence for spatial self-organization and its emergent effects in mussel bed ecosystems. Science 322, 739–742.

[45] Levin, S.A., 1992. The problem of pattern and scale in ecology: the Robert H. MacArthur award lecture. Ecology 73, 1943–1967.

[46] Levin, S.A., 1994. Patchiness in marine and terrestrial systems: from individuals to populations. Philos T R Soc B 343, 99–103.

[47] Levin, S.A., Powell, T.M., Steele, J.H., 1993. Patch dynamics lecture notes in biomathematics vol 96.

[48] Liu, Q.X., Doelman, A., Rottschäfer, V., de Jager, M., Herman, P.M., Rietkerk, M., van de Koppel, J., 2013. Phase separation explains a new class of self-organized spatial patterns in ecological systems. P Natl Acad Sci 110, 11905–11910.

[49] Liu, Q.X., Rietkerk, M., Herman, P.M., Piersma, T., Fryxell, J.M., van de Koppel, J., 2016. Phase separation driven by density-dependent movement: a novel mechanism for ecological patterns. Phys Life Rev 19, 107–121.

[50] Lloyd, M., 1967. Mean crowding. J Anim Ecol 36, 1–30.

[51] Lomax, K., 1954. Business failures: Another example of the analysis of failure data. J Am Stat Assoc 49, 847–852.

[52] Malchow, H., Petrovskii, S., Venturino, E., . Spatiotemporal Patterns in Ecology and Epidemiology: Theory, Models, and Simulations. 2008. Chapman and Hall, CRC, London.

[53] MATLAB, 2018. 9.4.0.813654 (R2018a). The MathWorks Inc., Natick, Massachusetts.

[54] McIntire, E.J., Fajardo, A., 2009. Beyond description: the active and effective way to infer processes from spatial patterns. Ecology 90, 46–56.

[55] Meron, E., 2015. Nonlinear physics of ecosystems. CRC Press.

[56] Mogilner, A., Edelstein-Keshet, L., Bent, L., Spiros, A., 2003. Mutual interactions, potentials, and individual distance in a social aggregation. J Math Biol 47, 353–389.

[57] Morisita, M., 1959. Measuring of the dispersion of individuals and analysis of the distributional patterns. Mem Fac Sci Kyushu Univ Ser E 2, 5–23.

[58] Morozov, A., Petrovskii, S., 2009. Excitable population dynamics, biological control failure, and spatiotemporal pattern formation in a model ecosystem. B Math Biol 71, 863–887.

[59] Murchie, A., Harrison, A., 2004. Mark-recapture of 'New Zealand flatworms' in grassland in Northern Ireland. Proc. Crop Protection in Northern Britain 2004 2526, 63–67.

[60] Nachman, G., 1981. Temporal and spatial dynamics of an acarine predator-prey system. J Anim Ecol 50, 435–451.

[61] Nathan, R., Getz, W.M., Revilla, E., Holyoak, M., Kadmon, R., Saltz, D., Smouse, P.E., 2008. A movement ecology paradigm for unifying organismal movement research. Proc Natl A Sci 105, 19052–19059.

[62] Neilson, E.W., Avgar, T., Burton, A.C., Broadley, K., Boutin, S., 2018. Animal movement affects interpretation of occupancy models from camera-trap surveys of unmarked animals. Ecosphere 9, e02092.

[63] Okamura, B., 1988. The influence of neighbors on the feeding of an epifaunal bryozoan. J Exp Mar Biol Ecol 120, 105–123.

[64] Okubo, A., 1986. Dynamical aspects of animal grouping: swarms, schools, flocks, and herds. Adv Biophys 22, 1–94.

[65] Okubo, A., Levin, S.A., 2013. Diffusion and ecological problems: modern perspectives. volume 14. Springer Science & Business Media.

[66] Parzen, E., 1962. On estimation of a probability density function and mode. Ann Math Stat 33, 1065–1076.

[67] Petrovskaya, N., Petrovskii, S., 2017. Catching ghosts with a coarse net: use and abuse of spatial sampling data in detecting synchronization. J R Soc Interface 14, 20160855.

[68] Petrovskaya, N., Petrovskii, S., Murchie, A.K., 2012. Challenges of ecological monitoring: estimating population abundance from sparse trap counts. J R Soc Interface 9, 420–435.

[69] Petrovskaya, N., Zhang, W., 2020. When seeing is not believing: Comparative study of various spatial distributions of invasive species. J Theor Biol 488, 110141.

[70] Petrovskaya, N.B., Forbes, E., Petrovskii, S.V., Walters, K.F., 2018. Towards the development of a more accurate monitoring procedure for invertebrate populations, in the presence of an unknown spatial pattern of population distribution in the field. Insects 9, 29.

[71] Petrovskii, S., Bearup, D., Ahmed, D.A., Blackshaw, R., 2012. Estimating insect population density from trap counts. Ecol Complex, 10, 69–82 .

[72] Petrovskii, S., Li, B.L., Malchow, H., 2004. Transition to spatiotemporal chaos can resolve the paradox of enrichment. Ecol Complex 1, 37–47.

[73] Petrovskii, S., Petrovskaya, N., Bearup, D., 2014. Multiscale approach to pest insect monitoring: Random walks, pattern formation, synchronization, and networks. Phys Life Rev, 11, 467–525 .

[74] Pimentel, D., Nagel, W., Madden, J.L., 1963. Space-time structure of the environment and the survival of parasite-host systems. Am Nat 97, 141–167.

[75] Piou, C., Berger, U., Hildenbrandt, H., Grimmb, V., Diele, K., D'Lima, C., 2007. Simulating cryptic movements of a mangrove crab: Recovery phenomena after small scale fishery. Ecol Model, 205, 110–122 .

[76] Pyke, G.H., 2015. Understanding movements of organisms: it's time to abandon the Lévy foraging hypothesis. Methods Ecol Evol 6, 1–16.

[77] Reynolds, A.M., Sinhuber, M., Ouellette, N.T., 2017. Are midge swarms bound together by an effective velocity-dependent gravity? Eur Phys J E 40, 46.

[78] Richner, H., Heeb, P., 1995. Is the information center hypothesis a flop? Adv Stud Behav 24, 1–46.

[79] Rosenblatt, M., 1956. Remarks on some nonparametric estimates of a density function. Ann Math Stat 27, 832–837.

[80] Satake, A., Iwasa, Y., 2000. Pollen coupling of forest trees: forming synchronized and periodic reproduction out of chaos. J Theor Biol 203, 63–84.

[81] Schmitz, O.J., Booth, G., 1997. Modelling food web complexity: the consequences of individual-based, spatially explicit behavioural ecology on trophic interactions. Evol Ecol 11, 379–398.

[82] Sih, A., 1984. The behavioral response race between predator and prey. Am Nat 123, 143–150.

[83] Skellam, J.G., 1951. Random dispersal in theoretical populations. Biometrika 38, 196–218.

[84] Swetnam, T.W., Lynch, A.M., 1993. Multicentury, regional-scale patterns of western spruce budworm outbreaks. Ecol Monogr 63, 399–424.

[85] Tagawa, Y., Mercado, J.M., Prakash, V.N., Calzavarini, E., Sun, C., Lohse, D., 2012. Three-dimensional Lagrangian Voronoï analysis for clustering of particles and bubbles in turbulence. J Fluid Mech 693, 201–215.

[86] Tilson, R.L., Hamilton III, W.J., 1984. Social dominance and feeding patterns of spotted hyaenas. Anim Behav 32, 715–724.

[87] Tirado, R., Pugnaire, F.I., 2003. Shrub spatial aggregation and consequences for reproductive success. Oecologia 136, 296–301.

[88] Turchin, P., 1998. Quantitative analysis of movement. Sinauer assoc. Sunderland (mass.).

[89] Tyutyunov, Y., Senina, I., Arditi, R., 2004. Clustering due to acceleration in the response to population gradient: a simple self-organization model. Am Nat 164, 722–735.

[90] Tyutyunov, Y.V., Zagrebneva, A., Surkov, F., Azovsky, A., 2009. Microscale patchiness of the distribution of copepods (Harpacticoida) as a result of trophotaxis. Biophysics 54, 355–360.

[91] Veresoglou, D., Fitter, A., 1984. Spatial and temporal patterns of growth and nutrient uptake of five co-existing grasses. J Ecol , 259–272.

[92] Viswanathan, G.M., Afanasyev, V., Buldyrev, S., Murphy, E., Prince, P., Stanley, H.E., 1996. Lévy flight search patterns of wandering albatrosses. Nature 381, 413.

[93] Viswanathan, G.M., Da Luz, M.G., Raposo, E.P., Stanley, H.E., 2011. The physics of foraging: an introduction to random searches and biological encounters. Cambridge University Press.

[94] Vulinec, K., Miller, M., 1989. Aggregation and predator avoidance in whirligig beetles *(Coleoptera: Gyrinidae)*. J New York Entomol S 97, 438–447.

[95] Wallin, H., 1988. The effects of spatial distribution on the development and reproduction of Pterostichus cupreus L., P. melanarius Ill., P. niger Schall. and Harpalus rufipes DeGeer (Col., Carabidae) on arable land. J Appl Entomol 106, 483–487.

[96] Wand, M.P., Jones, M.C., 1994. Kernel smoothing. Chapman and Hall/CRC.

[97] Wareing, D.R., 1986. Directional trail following in Deroceras reticulatum (Müller). J Mollus Stud 52, 256–258.

[98] Waters, W.E., 1959. A quantitative measure of aggregation in insects. J Econ Entomol 52, 1180–1184.

[99] Williams, J.C., ReVelle, C.S., Levin, S.A., 2005. Spatial attributes and reserve design models: a review. Environ Model Assess 10, 163–181.

[100] Wu, J., Loucks, O.L., 1995. From balance of nature to hierarchical patch dynamics: a paradigm shift in ecology. Q Rev Biol 70, 439–466.

Appendices

Appendix A. Auxiliary parameters in the model

Appendix A.1. The number of segments

In our model, we split a spatial domain within the perception radius into a number of segments to determine the direction of movement and we want to use the minimum number of segments possible. If the number of segments is exceedingly large, population clusters within the perception radius will be likely to be split up between several segments resulting in an incorrect conclusion about the mean angle as the variable m_s depends on S in (7). In addition,

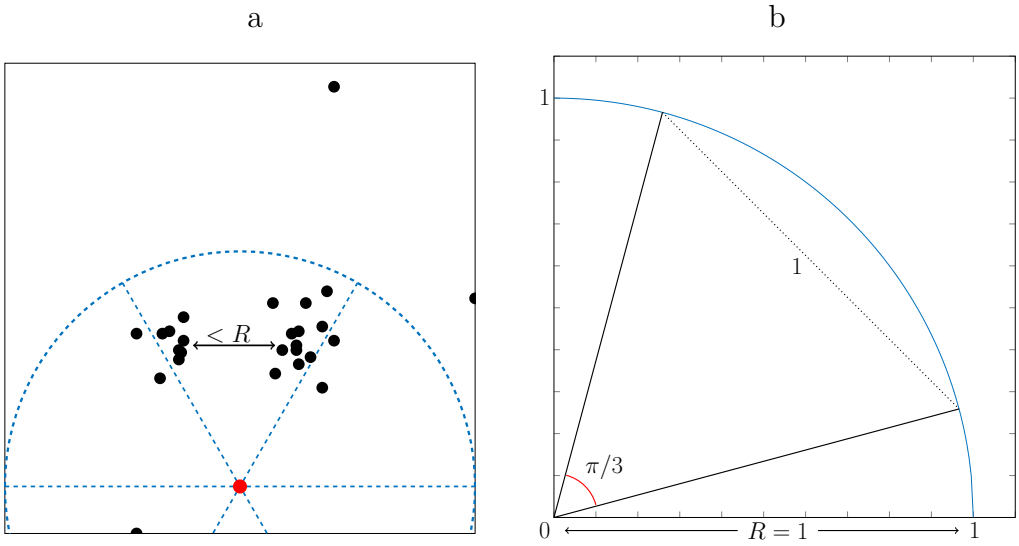

Figure A.23: *(a) the case where two clusters are contained within a single segment, (b) an illustration of a segment where that the largest distance between any two points within the segment is equal to R. The equilateral triangle shown for $R = 1$ has all angles equal to $\pi/3$.*

increasing the number of segments is more computationally expensive as the population has to be calculated for each segment within each animal's perception radius. On the other hand, if the number of segments is very small, we may have cases where two dense regions are positioned within the same segment (see Fig A.23(a)) and the direction the individual will move will be between the dense regions rather than towards either of them.

The minimum number of segments S_{min} required to control the directed movement in our model can be defined under the requirement that, when clusters form, they will have a distance between each other greater than the perception radius R (otherwise those areas are likely to be drawn together and coalesce). For two areas of high density to be in the same perception radius of an individual while not within the perception radius of each other, the minimum angle α_{min} between them from the location of the individual must be $\alpha_{min} = \pi/3$ radians; see Fig A.23(b). Hence, the minimum number of segments to guarantee that two clusters do not belong to the same segment is $S_{min} = 2\pi/\alpha_{min} = 6$ and we use the value of $S = 6$ in our simulations (cf. [62] where the authors use the same number of six 'neigbouring cells' around each animal in their simulation framework).

Let us emphasize that the number of segments is an auxiliary parameter introduced to help us to avoid any ambiguity in the choice of the direction of movement as discussed above. While any choice of $S \neq 0$ makes cluster formation more pronounced, S is not a critical parameter in the model. Clusters will form even if we use no segments at all because the parameter S is not present explicitly in the definition of the movement direction (7). The above statement is illustrated in Fig. A.24(a), where we compare the number of clusters formed when 6 segments are used in the model with that obtained in the model with no segments. As we can see from the figure, the difference between $S = 6$ and $S = 0$ is that, when we do not use segments, fewer clusters are formed on average. The difference in the mean number of clusters is immediate,

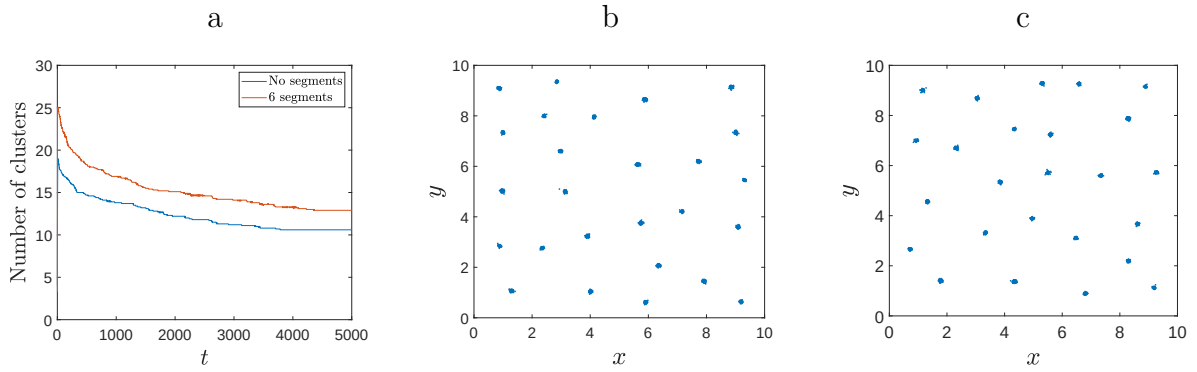

Figure A.24: *(a) The mean number of clusters formed in 10 simulations over 5000 time steps when* $S = 6$ *segments (solid red line) and no segments (solid blue line) are used in the model. (b, c) Example distributions at* $t = 10000$ *of Brownian walkers with movement parameters* $P = 0.6$, $R = 1$ *and* $\sigma = 0.02$. *(b) With 6 segments. (c) Without segments.*

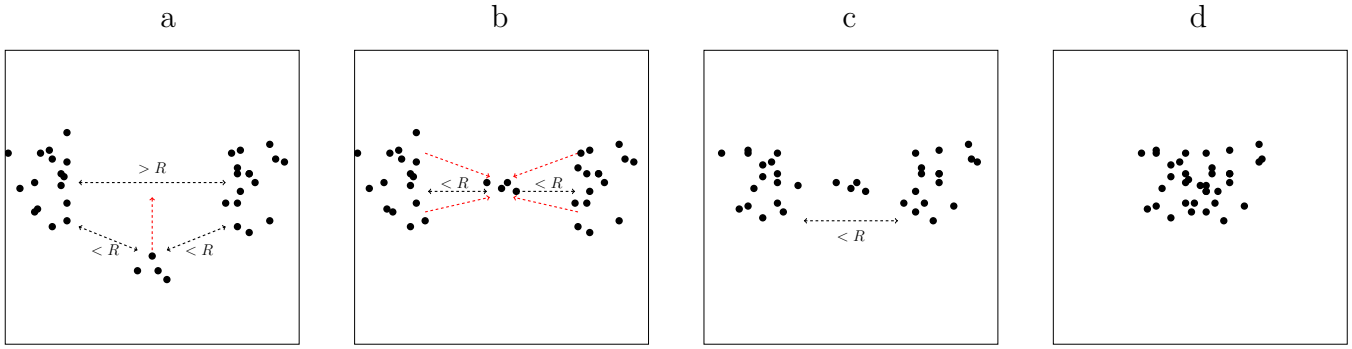

Figure A.25: *An illustration of how clusters may coalesce when influenced by individuals that move between clusters instead of towards them in a simulation without using segments. (a) A group of individuals have animals from two different clusters within their perception radius. They therefore move approximately along the direction of the red dotted line, in between the clusters. The two clusters are further than the perception radius apart. (b) As the free individuals move between the clusters, the individuals within clusters are influenced by the perception of the free individuals as they are within the perception radius. Therefore, both clusters shift slightly towards the centre. (c) The small shift in the position of the clusters has now put them within the perception radius of each other and they continue to move towards the centre. (d) The clusters will eventually coalesce into one.*

suggesting that this effect only happens in the first few time steps before clusters are fully formed. This could be because, when we do not use segments, it is more likely that an animal might move between two areas of high density rather than moving directly towards one if we use (7) to determine the directed movement in cases like that shown in Fig. A.25. In our opinion, such behaviour of an individual is an artefact of the model and it does not reflect biological traits of the population, hence we use the number of segments to alleviate that effect.

Interestingly, once the clusters have formed, their properties are similar in both cases $S \neq 0$ and $S = 0$. From the formation of clusters in Fig. A.24(a) and the example distributions in Fig. A.24(b)-(c) we can see that that there is very little difference in the spatial pattern of

	No Segments	$S = 4$	$S = 6$	$S = 12$
N_c	22.5	25.5	24.9	25.5
	(2.72)	(1.58)	(2.13)	(1.96)
$A_c \times 10^{-2}$	1.51	1.39	1.42	1.35
	(0.107)	(0.0519)	(0.0991)	(0.0598)
n_f	46.0	73.4	52.6	93.7
	(25.0)	(16.8)	(26.6)	(17.6)

Table A.12: *The mean and standard deviation of properties of clusters that are formed by Brownian walkers with different values of* S *at* $t = 10000$*, with movement parameters* $P = 0.6$*,* $R = 1$ *and* $\sigma = 0.02$*. The legend is the same as in Table 1. The values in the table are taken over* 10 *simulations.*

clusters produced or the time taken for the clusters to become 'stable'. These conclusions are further confirmed by results in Table A.12.

The orientation of segments is fixed for all animals in our model. It is possible that using randomly orientated segments for each time the angle of directed movement is calculated can reduce the effect of 'stretching' we discuss in Section 4. Further study of this problem is outside the scope of this paper but we believe that there would be no significant impact on the cluster properties that are key to our analysis.

Appendix A.2. The number of bins

The definition of a cluster that we have described in Section 2.2 requires splitting the domain into a certain number of bins. The number of bins used will have an effect on the cluster properties and we therefore want to examine how those properties change as we change the number of bins. Let us consider the cluster sizes when modelling with the normal distribution dispersal kernel. Table A.13 shows the cluster properties calculated using varying bin sizes. When the number of bins is 20^2 or higher, we have a constant number of clusters but the mean cluster area decreases and the number of free individuals increases as the number of bins increases. As this choice of parameters leads to dense clusters (see Fig. 6(d)), it is likely that all free individuals are very close to a cluster. When there is a large number of bins, it is more likely that these individuals will not be included as within a cluster because they occupy a bin that is slightly below the threshold.

In Fig. 3, we can see how the attributes of the clusters converge as we increase the number of bins. The number of clusters converges to a stable number for a number of bins just below 20x20 and the mean cluster population converges slightly earlier than that. In the case of a typical distribution generated by non-Brownian motion, shown in Fig. 5, the cluster properties shown in Fig. A.26 converge in a similar way but with some slight fluctuations to the number of clusters.

In deciding an appropriate bin size, it may be useful to analyse the distances between individuals in the field. The nearest neighbour method is a commonly used method in spatial analysis in ecology [25] and otherwise [5] where the mean and variance of the distances between a point and it's nearest individual are calculated. We can do a similar analysis and find the distance between every possible pair of individuals to show the spatial scales between and

	10^2	20^2	30^2	50^2	100^2
N_c	21.8	24.9	24.9	24.9	24.9
	(1.87)	(2.13)	(2.13)	(2.13)	(2.13)
$A_c \times 10^{-2}$	5.82	1.42	1.33	1.20	0.922
	(4.31)	(0.0991)	(0.0726)	(0.0704)	(0.0689)
n_f	33.2	52.6	108	216	470
	(14.5)	(16.5)	(30.4)	(37.7)	(80.7)

Table A.13: *The mean and standard deviation of properties of clusters that are formed by Brownian walkers with movement parameters* $P = 0.6$, $R = 1$ *and* $\sigma = 0.02$, *calculated using a different number of bins. The values in the table are taken over* 10 *simulations.*

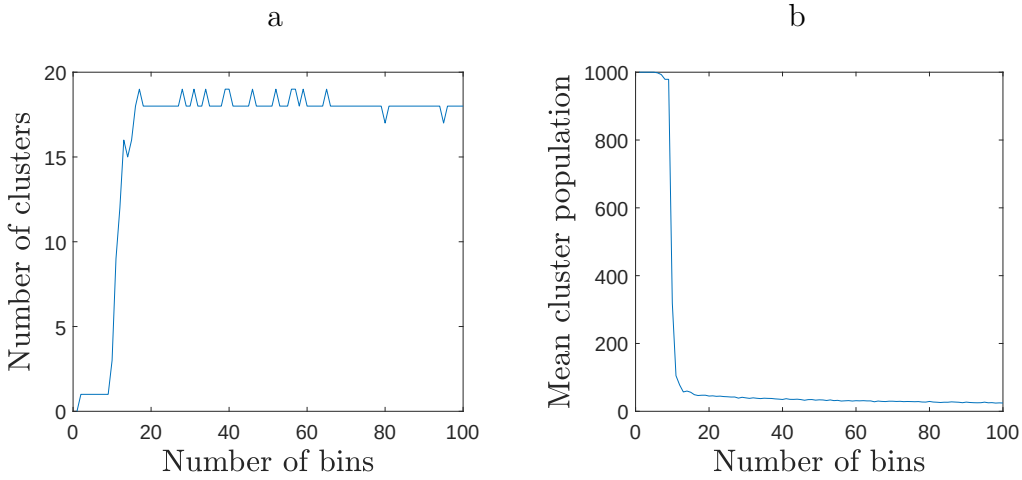

Figure A.26: *The cluster properties of a distribution of non-Brownian walkers as shown in the distribution in Fig. 5 when changing the number of bins.*

within clusters. We calculate the distances for the distributions as shown in Fig. 4 and Fig. A.27 shows the frequency with which different distances occur. Fig. A.27(a) shows a large amount of pairs have a distance close to 0, suggesting that those pairs are in the same cluster. Very few have a distance of length close to 1 and then the distance between pairs that are not in a cluster ranges from roughly 1.5 to 11.

Fig. A.27(b) shows the spike close to 0 in more detail. The distribution peaks at around 0.02 before decreasing to a level where there are only 10 distances measured between 0.15 and 0.2 and none at all between 0.2 and 1.1. This tells us that the diameter of the clusters are all less than 0.2 and also shows that clusters cannot be within a distance of 1 from each other, due to the perception radius R. The scales of distances within and between clusters can also explain the regions of stability in Fig. 3. We can see that the number of clusters and mean cluster population and area have a large shift between 5 and 15 bins, when the bin size is between 2 and 0.6, which the region where the minimum distance between clusters occurs.

The results are not so clear for the non-Brownian distribution as shown in Fig. A.27(c)-(d). Because of the amount of free individuals we do not have a range where no distances between

individuals occur. Fig. A.27(d) shows the minimum point in the distribution of distances is roughly 1.2 but, depending on our bin size, most of the distances in the region of 0.5 and 1.5 will be made up of distances where at least one of the individuals is free.

A grid of bins that would be sensible for both distributions would have to have bin sizes that are in the region $[0.1, 0.5]$ for the Brownian distribution. This is the region $[0.2, 1]$ halved as two neighbouring bins can make up part of the same cluster and so the distance over two bins should be restricted to this region. The non-Brownian case may require a slightly more restrictive region $[0.2, 0.5]$ but the results do not tell us as much as the Brownian distribution case.

Overall, from studying two example distributions generated from a random walk using either the normal distribution or the power law to generate the step size, we have enough information

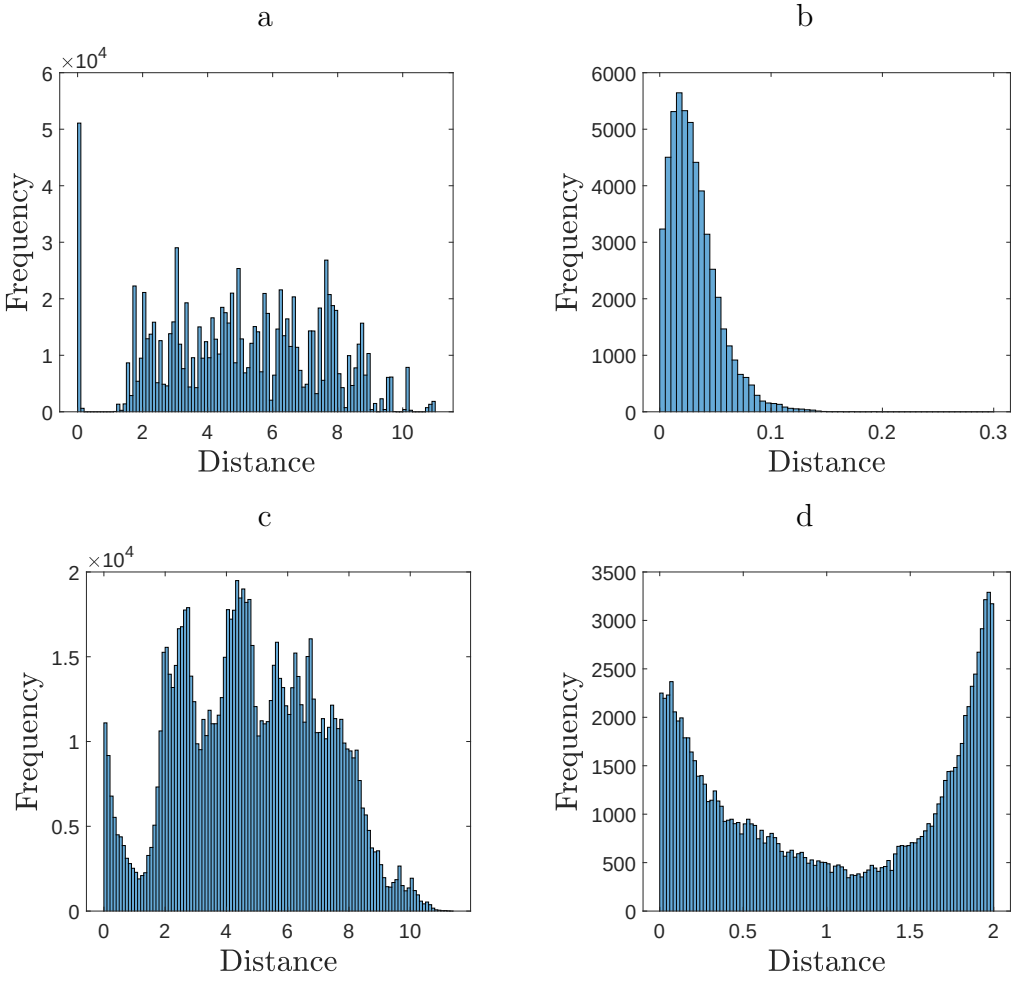

Figure A.27: *The frequencies of distances between individuals in the population distribution. The distance between every individual is calculated, giving* 1000^2 *data points. (a)-(b) Brownian walkers; see the distribution in Fig. 4(a) shows all distances, (b) shows the distances close to 0, i.e. for individuals within a cluster. (c)-(d) non-Brownian walkers; see the distribution in Fig. 5 (c) shows all distances, (d) shows the distances between 0 and 2, i.e. the area where pairs can be within a cluster, in neighbouring clusters or with individuals outside clusters.*

to justify a choice of the number of bins in the grid. In the Brownian case the properties of clusters are less sensitive to the change of bins than in the non-Brownian case but in both there is a region starting at slightly fewer than a grid of 20x20 bins, where there are not significant changes. Taking all the above information into account, we believe a 20x20 grid of bins is sufficient for analysing the properties of clusters.